Thermomechanical evolution of the crust during convergence and deep crustal pluton emplacement in the Western Province of Fiordland, New Zealand

Nathan R. Daczko

School of Geosciences, University of Sydney, NSW, Australia

Keith A. Klepeis

Department of Geology, University of Vermont, Burlington, Vermont, USA

Geoffrey L. Clarke

School of Geosciences, University of Sydney, NSW, Australia

Received 17 January 2001; revised 1 October 2001; accepted 14 December 2001; published 12 July 2002.

[1] Fiordland, New Zealand, contains exposures of high-pressure (P = 12–14 kbar) granulite facies rocks that form one of Earth's largest exposed lower crustal roots of an Early Cretaceous magmatic arc. These exposures allowed us to examine the mechanisms and processes that controlled crustal thickening and large vertical displacements at the deepest levels of a deforming arc system. We present structural and metamorphic data that show how the root of this arc was tectonically thickened by imbricate, granulite facies thrust zones during and after the emplacement of sheeted plutons into the middle and lower crust. The imbricate thrust zones form part of a well-exposed, 12 km wide, two-sided fold-thrust belt that preferentially developed in crust that was thermally softened by magmatism. Changes in metamorphic mineral assemblages and microstructural data from the contact aureole of a composite arc batholith called the Western Fiordland Orthogneiss record thrust and pluton emplacement conditions of $P \approx$ 7–9 kbar (paleodepths of 25–30 km). These data show that thrust imbrication and tectonic loading at 30 km depth is a viable mechanism of large vertical displacements and crustal thickening at the deepest levels of magmatic arcs. This mechanism produced a characteristic up-pressure metamorphic history that is similar to that observed in many other large magmatic belts worldwide. *INDEX TERMS:* 8015 Structural Geology: Local crustal structure; 8025 Structural Geology: Mesoscopic fabrics; 8005 Structural Geology: Folds and folding; 8102 Tectonophysics: Continental contractional orogenic belts; 8035 Structural Geology: Pluton emplacement; *KEYWORDS:* New Zealand, convergence, arc magmatism, lower crust, thrust tectonics

0278-7407/02/2001TC001282$12.00

1. Introduction

[2] Investigations of the exposed lower crustal roots of magmatic arcs are important for interpreting orogenic processes in arc settings and for understanding the environments where new continental crust is generated. However, many studies of tectonic processes in the deep crust are hindered by limited exposure of the lower crustal roots of arc systems [e.g., *Miller et al.*, 1993]. Two unresolved issues include the origin of up-pressure metamorphism in the deep crust of many arcs and the possible roles of contraction and thrust faulting during the thickening of arc-derived crust.

[3] Many previous investigations of arcs have shown that pluton emplacement occurs synchronously with regional tectonic activity and that this activity can involve contraction, extension, or different combinations of these and other tectonic styles. In the Coast Mountains Batholith of western North America, for example, some studies of arc tectonics emphasize extensional processes [*Klepeis and Crawford*, 1999; *Crawford et al.*, 1999], whereas others emphasize contraction [*Ingram and Hutton*, 1994; *Andronicos et al.*, 1999]. Other studies show that the tectonic environment in arcs can change periodically involving both extension and contraction (or transtension and transpression) at different stages [e.g., *Grocott et al.*, 1994; *Tobisch et al.*, 1995]. In some settings, displacements along ductile faults may influence pluton emplacement, especially in the deep crust [*Klepeis and Crawford*, 1999; *Crawford et al.*, 1999]. In other settings, buoyancy forces rather than regional stresses may control the ascent of magma [*Miller and Paterson*, 1999]. This diversity of process has created confusion about the roles of regional tectonic setting, thrust faulting, tectonic burial, and the interplay between thermal and deformational processes during arc evolution. The role of thrust faulting at the deepest levels of the Andean arc, for example, is uncertain because of lack of exposure. We address the roles of these processes at the deep levels of arc systems using a well-exposed batholith in Fiordland, New Zealand.

[4] Fiordland, New Zealand, contains Earth's largest (10,000 km^2) and best-exposed example of a young (Early

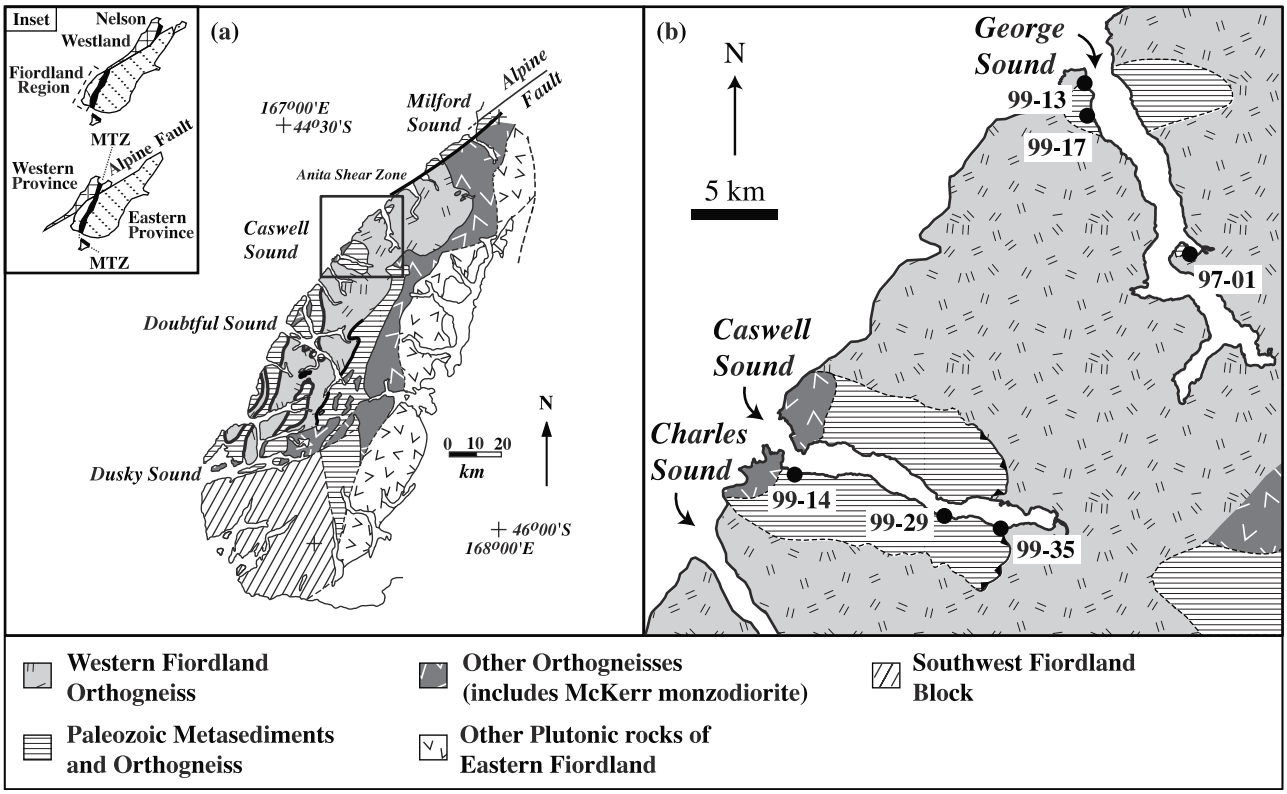

Figure 1. (a) Geological map of Fiordland showing major lithologic divisions (after *Bradshaw* [1990]). Inset shows pre-Cenozoic configuration of the South Island, which places the Westland/Nelson region adjacent to northern Fiordland (after *Hill* [1995a]). (b) Enlargement of George and Caswell Sounds showing the localities of key sites.

Cretaceous) granulite facies lower crustal root of a thickened (at least 45 km thick) magmatic arc [*Gibson et al.*, 1988; *Bradshaw*, 1990; *Oliver*, 1990; *Brown*, 1996]. However, despite excellent exposure and nearly three decades of study, interpretations of the tectonic environment in which the high-pressure, granulite facies rocks formed and the processes that affected them are controversial. Much of this controversy arises from conflicting interpretations of the origin, age, and significance of rock structures and a wide variety of metamorphic mineral assemblages within western Fiordland.

[5] One major source of discord among workers in Fiordland concerns the age of metamorphic assemblages and mineral zoning patterns in the high-grade rocks that indicate loading of the terrain [e.g., *Bradshaw*, 1989a; *Clarke et al.*, 2000]. This controversy is similar to one in the northern Cascades of the northwestern United States, where the origin and significance of up-pressure metamor-

Figure 2. (opposite) (a) Structural map of Caswell Sound showing major lithologic divisions and lines of cross sections. Thrust symbols on lines represent thrust zones that may be up to tens of meters wide. (b) Cross section (A–B) constructed for the southern shore of Caswell Sound showing S0/S1 foliation trajectories within the zone of polyphase folding and ductile shear. See text for discussion. (c) Cross section (A–C) constructed for the southern shore of Caswell Sound showing regional-scale variations in the orientation of foliations for the Caswell Sound fold-thrust belt. The section has been divided into four zones on the basis of structure. Inclined equals sign over a foliation trajectory indicates orthogneiss. Figures 2d–2g are lower hemisphere equal-area stereoplots of structural data from Caswell Sound. (d) Pre-fold-thrust belt structural elements ($L1^{CG}$ and poles to $S1^{CG}$) from the Caswell Gneiss west of the zone of imbricate thrust faults. (e) Pre-fold-thrust belt structural elements ($L1^{WFO}$ and poles to $S1^{WFO}$) from the Western Fiordland Orthogneiss east of the zone of imbricate thrust faults. (f) $D2^{CG}$ structural elements ($L2^{CG}$ and poles to $S2^{CG}$) from the Caswell Gneiss in the zones of polyphase folding and ductile shear and upright folding. (g) $D2^{ITF}$ structural elements ($L2^{ITF}$ and poles to $S2^{ITF}$) within the zone of imbricate thrust faults. Abbreviations are as follows: CG, Caswell Gneiss; ITF, imbricate thrust faults; WFO, Western Fiordland Orthogneiss. See text for discussion.

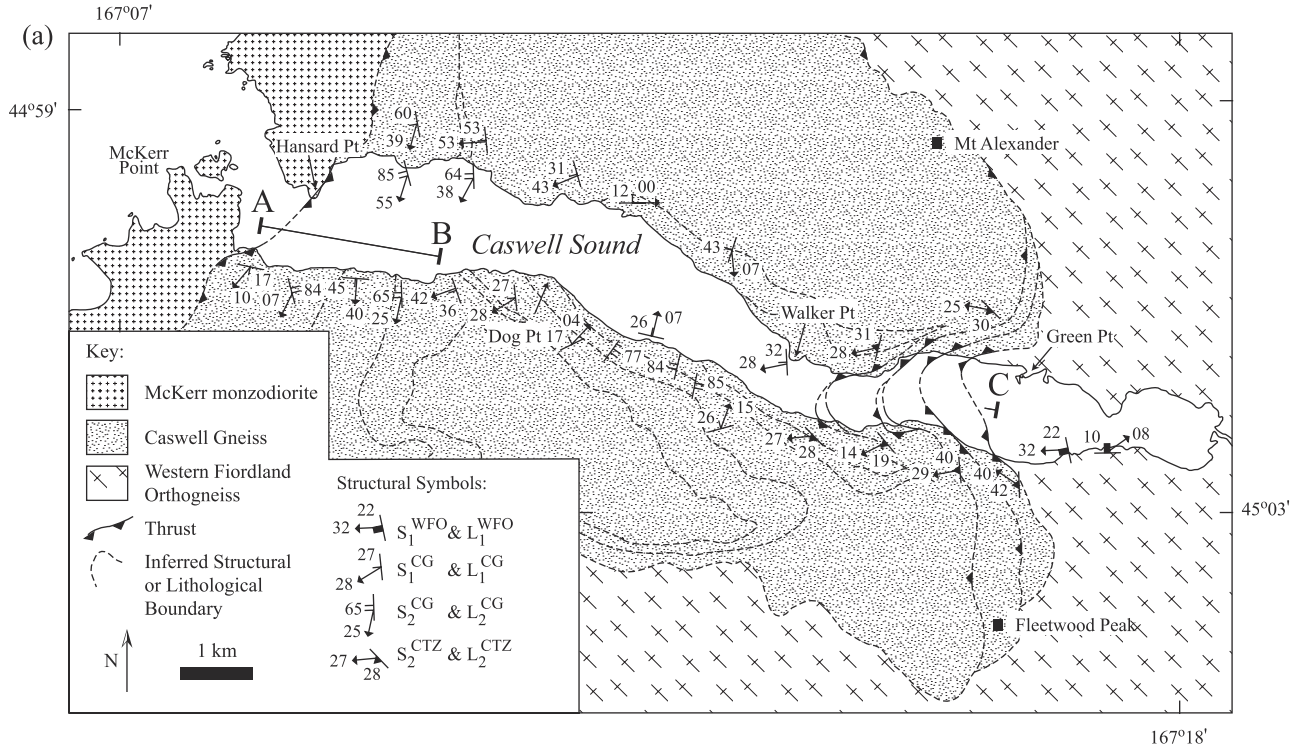
(a)
167°07'
44°59'
45°03'
167°18'
McKerr Point
Hansard Pt
Mt Alexander
Caswell Sound
Walker Pt
Green Pt
Dog Pt
Fleetwood Peak
A
B
C
Key:
McKerr monzodiorite
Caswell Gneiss
Western Fiordland Orthogneiss
Thrust
Inferred Structural or Lithological Boundary
N
1 km
Structural Symbols:
S1WFO & L1WFO
S1CG & L1CG
S2CG & L2CG
S2CTZ & L2CTZ

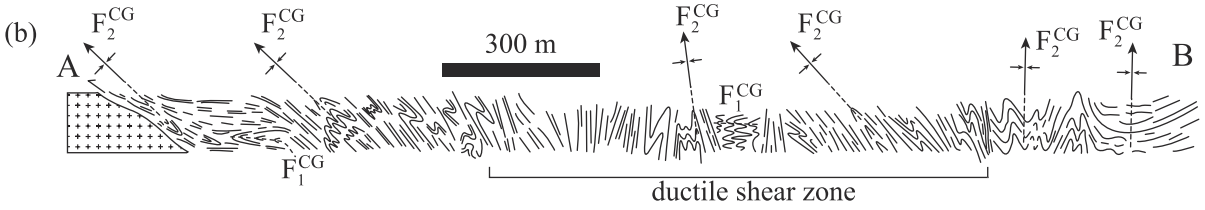
(b)
A
B
300 m
F2CG
F1CG
ductile shear zone

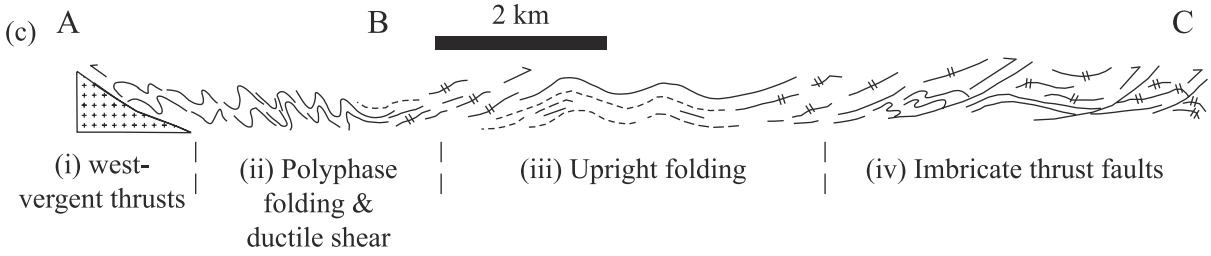
(c)
A
B
C
2 km
(i) west-vergent thrusts
(ii) Polyphase folding & ductile shear
(iii) Upright folding
(iv) Imbricate thrust faults

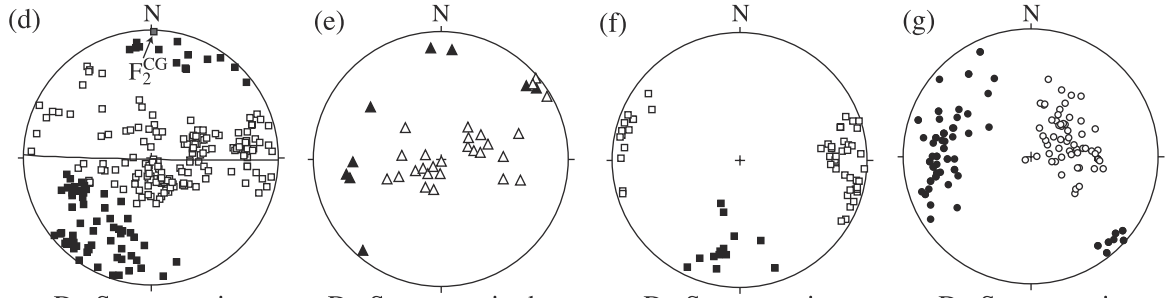
(d)
N
F2CG
D1 Structures in zones (ii) & (iii)
S1CG n = 40
L1CG n = 65
(e)
N
D1 Structures in the Western Fiordland Orthogneiss
S1WFO n = 27
L1WFO n = 11
(f)
N
D2 Structures in zone (ii)
S2CG n = 48
L2CG n = 13
(g)
N
D2 Structures in zone (iv)
S2ITF n = 57
L2ITF n = 48

phism is uncertain [*Miller et al.*, 2000]. High-pressure (where pressure (P) is 12–14 kbar) granulite facies assemblages are reported for Paleozoic paragneiss and the Cretaceous Western Fiordland Orthogneiss batholith, indicating that all units in Fiordland experienced a high-pressure event. However, the literature remains unclear on whether the arc batholith was emplaced into the middle to deep crust (P = 6–7 kbar) and loaded to the high-pressure metamorphic conditions during Cretaceous convergence [*Bradshaw*, 1989a; *Brown*, 1996] or whether the up-pressure metamorphic history is Paleozoic and the batholith was emplaced into the deep crust during extension [*Gibson et al.*, 1988; *Gibson and Ireland*, 1995].

[6] We have discovered field relationships at Caswell Sound that define a zone of intense folding and thrusting affecting the contact aureole of the Western Fiordland Orthogneiss arc batholith (Figures 1 and 2). Although previously hypothesized [*Oliver and Coggen*, 1979; *Bradshaw*, 1990], this find represents the first discovery of fold-thrust belt-type relationships within the western Fiordland arc rocks. It is especially significant because it allows us to test previously proposed models describing the significance of rock fabrics and the overall tectonic history of the Cretaceous arc batholith and country rocks that contain high-pressure (P = 12–14 kbar) garnet granulite facies assemblages (see *Clarke et al.* [2000] for a review). We show the importance of contractional tectonics on arc evolution, including burial, high-pressure metamorphism, and the P-T-t-D path of the terrain.

[7] In this paper we focus on relationships between deformation and metamorphism that followed the emplacement of the Western Fiordland Orthogneiss at Caswell Sound and discuss the significance of these relationships for interpreting the evolution of Fiordland's high-pressure granulite facies belt. We compare and contrast the fold-thrust belt setting with an undeformed intrusive contact at George Sound (Figure 1). We describe evidence of regional convergence and thrusting of Paleozoic paragneiss over the Western Fiordland Orthogneiss batholith at middle to lower crustal depths (~25–30 km). We conclude that the high-pressure granulite facies conditions were attained simultaneously with and at least in part due to tectonic loading, by the stacking of imbricated thrust sheets, during the Early Cretaceous. These new data show that models involving granulite emplacement wholly by Cretaceous extension or magmatic loading of this region are incomplete. Finally, we discuss the wider tectonic implications of this study to convergent margin tectonics, arc batholith emplacement, and associated contractional tectonics in general. We assess the potential significance of this research for interpreting processes affecting the deep levels of magmatic arcs.

2. Regional Geologic Setting

[8] The geology of the south island of New Zealand is divided into Eastern and Western provinces (inset Figure 1a) [*Landis and Coombs*, 1967; *Bishop et al.*, 1985]. A belt of rocks that is referred to as the Median Tectonic Zone (MTZ; inset Figure 1a) [*Kimbrough et al.*, 1993, 1994] or the Median Batholith [*Mortimer et al.*, 1999] separate these two provinces. Most of the Eastern Province formed within a convergent margin setting and contains arc-volcanic rocks, arc-derived sedimentary sequences, and accretionary complexes of Permian-Cretaceous age [*MacKinnon*, 1983; *Bradshaw*, 1989; *Mortimer*, 1995]. The Western Province contains extensive lower Paleozoic paragneiss (including the Caswell Gneiss of this study), cut by Devonian and Carboniferous granitoids [*Muir et al.*, 1996; *Wandres et al.*, 1998; *Ireland and Gibson*, 1998]. Rocks within this province preserve a polyphase mid-Paleozoic history that includes low-pressure/high-temperature metamorphism followed by medium-pressure/high-temperature metamorphism. Paleozoic events occurred when ancestral New Zealand lay within or outboard of the Pacific margin of Gondwana [*Wood*, 1972; *Carter et al.*, 1974; *Gibson and Ireland*, 1996; *Ireland and Gibson*, 1998; *Mortimer et al.*, 1999].

[9] The Median Tectonic Zone is a comparatively narrow belt of tectonically disrupted arc-related rocks with U-Pb zircon ages that mostly fall into two age groups: 247–195 Ma and 157–131 Ma (Figure 1) [*Bradshaw*, 1993; *Kimbrough et al.*, 1993, 1994]. Late Triassic Median Tectonic Zone plutons that intrude the Eastern Province indicate that this province and the tectonic zone were together at this time [*Williams and Harper*, 1978; *Mortimer et al.*, 1999]. Rocks of the Median Tectonic Zone and the Western Province are intruded by stitching plutons of the Early Cretaceous Western Fiordland Orthogneiss/Separation Point Suite (Figure 1) [*Bradshaw*, 1990; *Kimbrough et al.*, 1994].

[10] The Western Fiordland Orthogneiss (WFO; Figure 1) [*Bradshaw*, 1990] is a batholithic-scale unit of mafic to intermediate composition that was emplaced into thickened arc crust. Maximum pressures for Fiordland crust indicate that the arc was at least 45 km thick during the Early Cretaceous, and geophysical studies of the present-day crustal structure suggest that at least a further 10 km of crust still lies beneath Fiordland [*Oliver*, 1990]. Conventional and sensitive high-resolution ion microprobe (SHRIMP) U-Pb zircon ages range between 126 and 116 Ma [*Mattinson et al.*, 1986; *Gibson et al.*, 1988; *Gibson and Ireland*, 1995; *Muir et al.*, 1998]. Amphibolite facies shear zones juxtapose the Western Fiordland Orthogneiss with Paleozoic paragneiss to the northwest, west, and south (Figure 1) [*Gibson et al.*, 1988; *Hill*, 1995a, 1995b; *Klepeis et al.*, 1999]. George Sound and Mt Daniel (Figure 1) preserve relationships where the Western Fiordland Orthogneiss intrudes Paleozoic paragneiss and the Arthur River Complex orthogneiss, respectively [*Bradshaw*, 1990]. Contact relationships with rocks of the Eastern Province are mostly intrusive but are poorly understood [*Bradshaw*, 1990].

[11] *Ireland and Gibson* [1998] observed changes in metamorphic assemblages and used microprobe U-Pb dating of zircon/monazite to infer loading of Paleozoic paragneiss from P = 3–5 kbar to P = 7–9 kbar between 360 Ma and 330 Ma. These authors also examined Cretaceous shear zones in the Doubtful Sound region (Figure 1) and inferred

the emplacement of the Western Fiordland Orthogneiss, during regional extension, into rocks that were already at lower crustal conditions ($P > 12$ kbar).

[12] In contrast, *Bradshaw* [1989b, 1990] and *Bradshaw and Kimbrough* [1989] used conventional U-Pb zircon dating [*Mattinson et al.*, 1986] and estimates of metamorphic *P-T* paths to infer the midcrustal emplacement of the Western Fiordland Orthogneiss batholith coeval with low- to medium-pressure ($P = 6–7$ kbar) granulite facies metamorphism. A substantial increase in pressure (to $P = 12–13$ kbar) and the subsequent formation of garnet granulite throughout Fiordland was attributed by these authors to tectonic burial consequent to regional convergence (possibly involving arc-continent collision). In contrast, using petrographic analyses and field data reported by *Bradshaw* [1989a, 1989b, 1990], *Oliver* [1990], and *Brown* [1996] inferred that the high-pressure granulite facies conditions were produced by magma loading following emplacement of the Western Fiordland Orthogneiss at midcrustal conditions. Finally, *Muir et al.* [1995, 1998] used geochemical and geochronologic data to argue that an Early Cretaceous magmatic arc, chemically equivalent to parts of the Median Tectonic Zone, was thrust beneath western Fiordland during convergence to depths in excess of 40 km and melted to produce the Western Fiordland Orthogneiss. It is therefore unclear within the literature whether a dominantly convergent or extensional tectonic setting accompanied formation of the Fiordland high-pressure granulites and what caused the loading of these rocks. The exhumation of parts of the Fiordland high-pressure metamorphic belt has been attributed to latest Cretaceous crustal extension, prior to the opening of the Tasman Sea Basin [*Gibson et al.*, 1988], supplemented by early to late Cenozoic transpressive motion in northern Fiordland [*Blattner*, 1991; *Klepeis et al.*, 1999].

3. Rock Units

[13] From east to west, Caswell Sound contains three main rock types: (1) Western Fiordland Orthogneiss, (2) Caswell Gneiss, and (3) McKerr monzodiorite (Figure 2a). The Western Fiordland Orthogneiss is most commonly weakly deformed hornblende-plagioclase-dominated gabbroic gneiss. However, two-pyroxene gabbroic gneiss and K-feldspar-quartz monzogranite varieties occur at some localities. Tabular plagioclase laths sharing long, straight grain boundaries with pyroxene or amphibole are relict igneous textures.

[14] The Caswell Gneiss consists of 60% paragneiss and 40% biotite dioritic orthogneiss. The paragneisses are best exposed along the shores of Caswell Sound at its western end near the contact with the McKerr monzodiorite (Figure 2a). The paragneiss comprises calc-silicate and mafic gneiss, marble, and metapsammitic schist. All units are interbedded, and the thickness of sedimentary layering is highly variable ranging from a few centimeters to more than 100 m. The biotite-plagioclase-dominated dioritic orthogneiss contains rafts of the paragneiss and is best exposed near Walker Point (Figure 2a). The orthogneiss forms sill-like intrusions that appear to be more than 500 m thick.

[15] The McKerr monzodiorite is a very weakly deformed biotite-plagioclase rock that cuts the Caswell Gneiss. The contact with Caswell Gneiss displays clasts of brecciated paragneiss within the monzodiorite that are inferred to represent an igneous breccia. This contact is tectonized as discussed in section 4.5 (Figure 2b).

[16] George Sound contains Western Fiordland Orthogneiss that envelops and cuts rafts of intensely foliated schists of the Paleozoic George Sound Paragneiss that may be up to 4 km wide (site 97-17; Figure 1b) [*Bradshaw*, 1990]. Diatexite zones (up to 200 m wide) occur at the contacts between the George Sound Paragneiss and the Western Fiordland Orthogneiss (site 97-01 and 97-13; Figure 1b). The George Sound Paragneiss is most probably equivalent to the metasedimentary units of the Caswell Gneiss, though no marble horizons were observed at George Sound.

4. Geometry and Fabric Elements of the Caswell Fold-Thrust Belt

[17] Caswell Sound contains ~12 km of continuous exposure across a fold-thrust belt that deforms the upper contact of the Early Cretaceous Western Fiordland Orthogneiss batholith (Figure 2). We divide the section into six structural domains. From east to west, these include (1) a weakly deformed Western Fiordland Orthogneiss, (2) a zone of gently west dipping imbricate thrust faults that deform the contact between the Western Fiordland Orthogneiss and Caswell Gneiss, (3) a zone characterized by upright folds and no thrust zones, (4) a zone of polyphase folding and ductile shear, (5) a zone of west vergent thrusting at the contact between the Caswell Gneiss and the McKerr monzodiorite, and (6) weakly deformed to undeformed McKerr monzodiorite. In this section we define the geometry and structural elements of the fold-thrust belt, including the mineral assemblages within each domain.

4.1. Structural Elements Deformed by the Caswell Fold-Thrust Belt

[18] The Western Fiordland Orthogneiss and McKerr monzodiorite to the east and west of the Caswell Gneiss, respectively, were weakly to very weakly deformed prior to the development of the fold-thrust belt. The Western Fiordland Orthogneiss displays a weakly developed foliation ($S1^{WFO}$) that is most probably a reworked magmatic foliation. $S1^{WFO}$ is commonly defined by aligned and elongate clusters of mafic minerals in a dominantly feldspar matrix. Mafic mineral clusters most commonly comprise coarse calcic-amphibole and clinozoisite with or without biotite and rutile. In some localities, the mafic mineral clusters are cored by coarse orthopyroxene and clinopyroxene rimmed by fine amphibole. At these localities, orthopyroxene and clinopyroxene grains exhibit magmatic textures defined by coarse, equant orthopyroxene aggregates with exsolution blebs of clinopyroxene and opaque phases. The orientation of $S1^{WFO}$ is variable displaying both steep and shallow dips

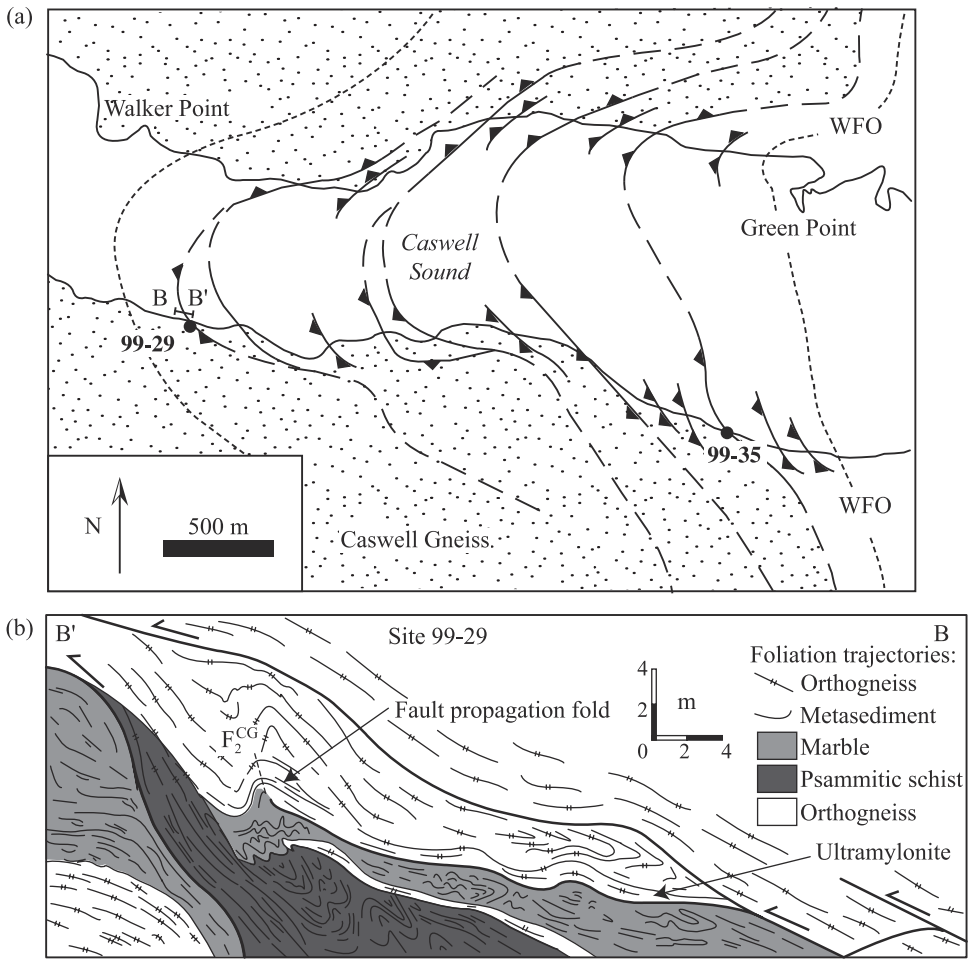

Figure 3. (a) Structural map of the zone of imbricate thrust faults. Boundaries of the zone of imbricate thrust faults are shown as fine dashed lines. Thrust symbols on lines represent thrust zones that may be up to tens of meters wide as detailed in Figure 3b. Note that thrust zones cut the Western Fiordland Orthogneiss. (b) Vertical section B-B′ shown in Figure 3a of a thrust zone in the Caswell Gneiss viewed perpendicular to transport direction. Note zones of ultramylonite and fault propagation folds.

(Figure 2e). On the basis of limited lineation data, a weakly developed amphibole mineral lineation ($L1^{WFO}$) shallowly plunges variably to the north, northeast, and west (Figure 2e). The McKerr monzodiorite shows randomly oriented biotite and feldspar with no evidence of a foliation or a lineation.

[19] Within the Caswell Gneiss, the dominant pre-fold-thrust belt structure is a well-developed shallowly dipping foliation ($S1^{CG}$) that subparallels bedding planes in paragneiss and parallels the margins of sills within the biotite diorite. Foliated rafts of metasediment within the biotite diorite suggest that the paragneiss experienced a complex pre-fold-thrust belt history that, for simplicity, we omit here. The $S1^{CG}$ foliation is defined by lenticular aggregates of quartz and feldspar and aligned muscovite, biotite, or chlorite grains. This foliation is axial planar to recumbent, isoclinal folds of bedding (Figure 2b). The foliation planes contain a well-developed shallowly SSW plunging muscovite and biotite mineral lineation (Figure 2d). The axial planar $S1^{CG}$ foliation and recumbent folds are folded by upright, gently south plunging $F2^{CG}$ folds (Figure 2b), such that the early folds are no longer recumbent in many places.

4.2. Zone of Imbricate Thrust Faults (ITF)

[20] The zone of imbricate thrust faults extends westward from Green Point within the Western Fiordland Orthogneiss to Walker Point within the Caswell Gneiss (Figure 3a). A traverse westward along Caswell Sound from Green Point shows ~10 shallowly west dipping outcrop-scale thrust zones that display listric geometries. The thrust zones cut the Western Fiordland Orthogneiss, the contact aureole proximal to the Western Fiordland Orthogneiss, and the Caswell Gneiss foliation outside the contact aureole. The thrust zones consist of narrow (<250 m wide) zones of highly deformed and recrystallized Western Fiordland Orthogneiss and/or Caswell Gneiss. The spacing between fault zones is ~200–400 m. Well-developed foliations ($S2^{ITF}$) in the thrust zones are locally

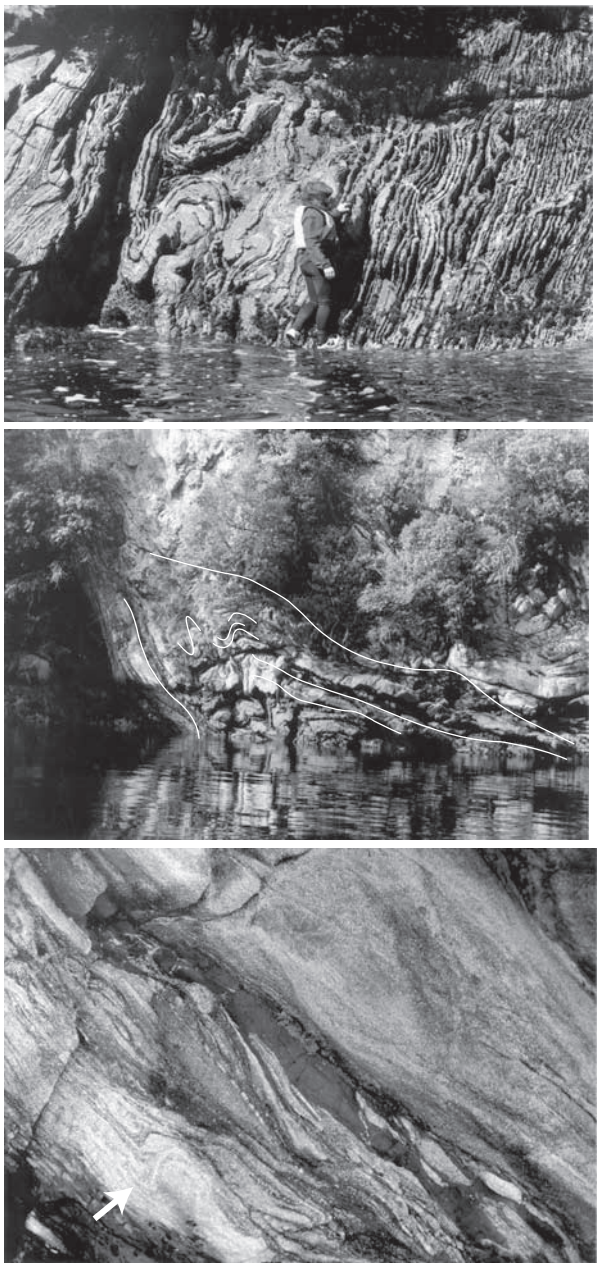

Figure 4. (a) Outcrop photograph of a well-developed, steeply dipping $S2^{CG}$ foliation that is axial planar to $F2^{CG}$ folds of a composite S0/S1 in the zone of polyphase folding and ductile shear (view to south). Person for scale. (b) Outcrop photograph showing $D2^{ITF}$ thrust zone in the Caswell Gneiss (view to south). This outcrop was the source for Figure 3b. Person for scale. (c) Outcrop photograph showing $D2^{ITF}$ thrust zone in the Western Fiordland Orthogneiss (view to south). Marker pen (~13 cm long) for scale.

mylonitic to ultramylonitic. $S2^{ITF}$ foliation planes contain well-developed mineral lineations that plunge gently to the west (Figures 2g, 4b and 4c). The ultramylonitic bands show small ramp-flat geometries that include curvatures in the fault surfaces (Figure 3b). Thrust zones are most commonly found in rheologically weak zones that include the contact between Western Fiordland Orthogneiss and country rock and marble layers (Figure 3b). Approximately 80% of the imbricate thrust zones are located within thin marble horizons. In many cases it is unclear whether the marbles are interbeds or thrust zone slices. At least some of the marble horizons contain less-deformed boundaries and are thick enough to suggest they represent original bedding horizons. Figure 3b shows common features of individual thrust zones. These include fault propagation folds [*Suppe*, 1985] that accommodate fault displacement where ultramylonitic ramps terminate. Folds ($F2^{ITF}$) of compositional layering, $S1^{CG}$, and $S1^{WFO}$ between individual thrust zones are commonly rootless with axial planes that lie parallel to the shallow to moderately west dipping mylonitic to ultramylonitic folia (Figures 3b, 4b and 4c).

[21] Western Fiordland Orthogneiss in contact with the Caswell Gneiss is a monzogranite. It has the $S2^{ITF}$ assemblage garnet, biotite, plagioclase, K-feldspar, and quartz with or without muscovite, titanite, and hematite. At most other localities the Western Fiordland Orthogneiss is dioritic to gabbroic gneiss with a similar assemblage that lacks garnet. Thrust zones that deform Caswell Gneiss within 500 m of the contact with the Western Fiordland Orthogneiss contain the $S2^{ITF}$ assemblage garnet, biotite, plagioclase, K-feldspar, and quartz in biotite diorite and psammitic schist. Thrust zones in the Caswell Gneiss more than 500 m and up to 2.5 km from the contact with the Western Fiordland Orthogneiss contain the $S2^{ITF}$ assemblage chlorite, muscovite, and quartz with porphyroclasts of plagioclase, K-feldspar, clinozoisite, and amphibole in biotite diorite and psammitic schist.

4.3. Zone of Upright Folding

[22] For ~4 km west of the imbricate thrust zones, $S1^{CG}$ is deformed by open to tight, upright $F2^{CG}$ folds of the sheeted biotite dioritic orthogneiss (Figures 2b and 2c). These folds deform the early shallowly dipping foliation ($S1^{CG}$) and sills of biotite diorite in the Caswell Gneiss. A well-developed foliation ($S2^{CG}$,; Figure 4a) formed axial planar to the $F2^{CG}$ folds. The assemblage garnet, biotite, muscovite, chlorite, plagioclase, and quartz most commonly defines $S2^{CG}$ in metapelitic schists. In this zone of upright folding, $S2^{CG}$ foliation planes strike north and dip steeply to the east and west (Figures 2f and 4a). $S2^{CG}$ foliation planes contain a well-developed mineral lineation, defined mostly by biotite and muscovite that plunges shallowly to the south, subparallel to $F2^{CG}$ fold axes. At the eastern boundary of this zone (near Walker Point), $S2^{CG}$ foliation planes gradually dip more gently to the west to lie parallel to the shallow to moderately west dipping $S2^{ITF}$ foliation planes of the imbricate thrust zone.

4.4. Zone of Polyphase Folding and Ductile Shear

[23] West of the zone of upright folding is a 3–4 km wide zone of polyphase, tight folding, and ductile shear. The

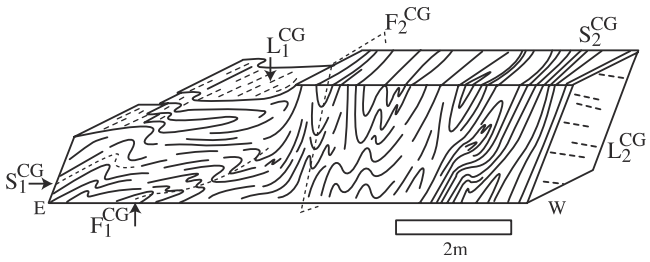

Figure 5. Sketch of foliation and superposed fold relationships in the zone of polyphase folding and ductile shear.

eastern boundary of this zone is gradational from the zone of upright folding across ~500 m where folds become tighter westward. The western boundary of this zone is a west vergent thrust near Hansard Point (Figure 2a). The most distinguishing feature of this zone is a 1.5-km-wide ductile shear zone that deforms a succession of calc-silicate, metapelitic, psammitic, and marble units. The shear zone is characterized by upright, asymmetric, tight to isoclinal folds and a very well-developed steeply dipping foliation ($S2^{CG}$; Figures 4a and 5). This shear zone foliation crosscuts all early shallowly dipping foliations and recumbent folds in the Caswell Gneiss. The tight upright folds are coaxial with the older recumbent folds and produce a macroscopic type-3 interference pattern (fishhooks). With the exception of an area of "M-type" symmetrical fold geometry in the central region of this zone, most of these folds are overturned and west vergent (Figures 2b and 2c). Proximal to the zone of west vergent thrusting, the near vertical axial planes of these $F2^{CG}$ folds become inclined and subparallel the west vergent thrusts (Figure 2b).

4.5. Zone of West Vergent Thrusting

[24] A zone of west vergent thrusting is defined by a narrow (<50 m) series of semi-brittle, east-dipping thrust zones that separate the most highly deformed part of the section (the ductile shear zone described in the previous section) from the weakly deformed McKerr monzodiorite. The narrow width of the west vergent thrust zone and the small number of thrusts within it suggest that this style and direction of thrusting is subordinate to the more abundant east vergent thrust zones in the imbricate zone.

5. Comparison of Western Fiordland Orthogneiss Contact Relations: Caswell Sound Versus George Sound

[25] Caswell Sound contains exposures of the upper (southwestern) contact of the Western Fiordland Orthogneiss batholith. George Sound preserves a 4-km-wide section of metasedimentary rock that is wholly enveloped by the Western Fiordland Orthogneiss. We infer that George Sound exposes rock structurally below the upper contact preserved at Caswell Sound. Patterns of deformation observed at George Sound differ in style and intensity from those described above for Caswell Sound. A well-preserved diatexite and a weakly deformed contact zone suggest that the contact aureole at George Sound was shielded from most of the effects of Early Cretaceous contractional deformation. The absence of thrust zones or other intense contractional deformation at George Sound suggests that Early Cretaceous deformation was partitioned into the upper contact at Caswell Sound where weak, thermally softened marble and calc-silicate horizons localized thrust zones at the Western Fiordland Orthogneiss boundary.

6. Metamorphism and Conditions of Deformation

[26] In this section we present calculated temperature and pressure conditions from the metamorphic assemblages outlined below. Finally, we present evidence for a 500-m-wide thermal gradient in the contact aureole of the Western Fiordland Orthogneiss at Caswell Sound using variations in metamorphic mineral assemblage and quartz and feldspar microstructures.

6.1. Calculated Pressure and Temperature Conditions

[27] The $S1^{CG}$ mineral assemblage within the Caswell Gneiss includes garnet, amphibole, biotite, plagioclase, and quartz. At George Sound foliated schists in country rock outside the diatexite zone contain the assemblage garnet, kyanite, biotite, staurolite, plagioclase, and quartz. On the basis of crosscutting relationships we infer that these assemblages and the foliations they define formed prior to emplacement of the Western Fiordland Orthogneiss.

[28] The high-grade thrust zones within and near the Western Fiordland Orthogneiss contact at Caswell Sound (site 99-35; Figure 1b) contain foliations defined by the metamorphic assemblage garnet, biotite, plagioclase, K-feldspar, and quartz. Thrust zones more than 500 m from the contact with the Western Fiordland Orthogneiss (site 99-29; Figure 1b) do not contain assemblages suitable for calculating metamorphic conditions. However, garnet-bearing $S2^{CG}$ assemblages occur in metapelitic schists in the zone of polyphase folding and ductile shear (site 97-14; Figures 1b, 2c, and 4a). These assemblages are inferred to have formed synchronously with those in the zone of imbricate thrust faults on the basis of a correlation of $S2^{CG}$ and $F2^{CG}$ structures across Caswell Sound, a lack of crosscutting relationships between these structures across structural domains, and similar conditions of metamorphism (e.g., sites 97-14 and 97-29; Figure 1b).

[29] We use the assemblages outlined above to estimate metamorphic temperature and pressure paths prior to and during development of the Caswell fold-thrust belt. We also calculate *P-T* conditions that accompanied $D2^{CG}/D2^{ITF}$ and compare these temperatures with estimates obtained using microstructures. Representative microprobe analyses of equilibrium assemblages are presented in Table 1a. We used directly calibrated thermometry [*Ferry and Spear*, 1978; *Graham and Powell*, 1984] and the average *P-T* approach using the computer software THERMOCALC (version 2.6) [*Powell and Holland*, 1988] (Table 1b). For average *P-T*

Table 1a. Representative Microprobe Analyses (wt % Oxide and Cation Data) of Selected Equilibrium Assemblages[a]

	George Sound Diatexite Sample 97-01J2				$S2^{CG}$ (Zone of Polyphase Folding and Ductile Shear) Sample 99-14A						$S2^{TZ}$ (Zone of Imbricate Thrust Faults-Caswell Gneiss) Sample 99-35				$S2^{ITZ}$ (Zone of Imbricate Thrust Faults-WFO) Sample 99-35D			
	g	bi	amph	pl	g	bi	mu	pl	ep	chl	g	bi	pl	ksp	g	bi	pl	ksp
SiO_2	36.95	35.23	39.29	63.19	36.68	34.22	45.06	59.47	37.98	24.72	36.77	35.64	58.27	64.91	36.84	34.69	62.06	63.95
TiO_2	0.06	2.47	0.73	0.01	0.08	1.66	0.65	0.02	0.07	0.09	0.01	2.52	0.00	0.03	0.03	3.12	0.02	0.00
Al_2O_3	20.72	15.91	14.26	22.89	21.24	18.49	34.53	25.75	26.98	21.83	21.22	17.75	26.24	18.16	20.43	15.90	23.87	18.83
Cr_2O_3	0.02	0.02	0.08	0.00	0.00	0.04	0.00	0.00	0.00	0.00	0.03	0.02	0.02	0.00	0.00	0.03	0.08	0.00
FeO	28.62	21.34	21.97	0.17	26.79	22.34	2.60	0.04	9.02	26.59	32.91	18.96	0.10	0.03	28.33	26.62	0.02	0.08
MnO	4.24	0.13	0.30	0.01	8.46	0.17	0.00	0.00	0.36	0.36	3.05	0.11	0.03	0.00	5.09	0.42	0.03	0.00
MgO	1.98	9.21	6.08	0.00	1.71	9.25	0.56	0.01	0.01	15.14	2.95	9.26	0.02	0.02	1.44	5.03	0.01	0.02
CaO	7.41	0.01	10.19	4.08	4.84	0.04	0.00	7.02	23.25	0.01	3.40	0.00	8.16	0.00	7.51	0.00	5.06	0.03
Na_2O	0.09	0.17	2.31	9.31	0.03	0.18	0.90	7.53	0.01	0.03	0.02	0.11	6.97	0.19	0.06	0.03	8.58	0.87
K_2O	0.01	9.26	1.24	0.09	0.00	9.55	10.02	0.06	0.01	0.02	0.02	9.45	0.07	16.32	0.01	9.55	0.21	15.91
Total	100.09	93.76	96.44	99.74	99.82	95.95	94.32	99.90	97.68	88.79	100.38	93.83	99.87	99.64	99.73	95.38	99.93	99.69
# O	12	22	23	8	12	22	22	8	25	28	12	22	8	8	12	22	8	8
Si	3.0	5.5	6.2	2.8	3.0	5.3	6.1	2.7	6.1	5.2	3.0	5.5	2.6	3.0	3.0	5.5	2.8	3.0
Ti	0.0	0.3	0.1	0.0	0.0	0.2	0.1	0.0	0.0	0.0	0.0	0.3	0.0	0.0	0.0	0.4	0.0	0.0
Al	2.0	2.9	2.6	1.2	2.0	3.4	5.5	1.4	5.1	5.4	2.0	3.2	1.4	1.0	2.0	3.0	1.2	1.0
Cr	0.0	0.0	0.0	0.0	0.0	0.0	0.0	0.0	0.0	0.0	0.0	0.0	0.0	0.0	0.0	0.0	0.0	0.0
Fe	1.9	2.8	2.9	0.0	1.8	2.9	0.3	0.0	1.2	4.7	2.2	2.5	0.0	0.0	1.9	3.5	0.0	0.0
Mn	0.3	0.0	0.0	0.0	0.6	0.0	0.0	0.0	0.0	0.1	0.2	0.0	0.0	0.0	0.3	0.1	0.0	0.0
Mg	0.2	2.2	1.4	0.0	0.2	2.1	0.1	0.0	0.0	4.7	0.4	2.1	0.0	0.0	0.2	1.2	0.0	0.0
Ca	0.6	0.0	1.7	0.2	0.4	0.0	0.0	0.3	4.0	0.0	0.3	0.0	0.4	0.0	0.7	0.0	0.2	0.0
Na	0.0	0.1	0.7	0.8	0.0	0.1	0.2	0.7	0.0	0.0	0.0	0.0	0.6	0.0	0.0	0.0	0.7	0.1
K	0.0	1.9	0.2	0.0	0.0	1.9	1.7	0.0	0.0	0.0	0.0	1.9	0.0	1.0	0.0	1.9	0.0	0.9
Total	8.0	15.7	15.9	5.0	8.0	15.8	14.1	5.0	16.4	20.1	8.0	15.5	5.0	5.0	8.0	15.6	5.0	5.0

[a] Data were obtained using a Cameca SX50 microprobe housed at the University of New South Wales running at an accelerating voltage of 15 kV and a beam width of 1–5 m.

Table 1b. Directly Calibrated Thermometry, Average *P-T* Calculations of Selected Equilibrium Assemblages[a]

Method	George Sound Diatexite Sample 97-01J2	$S2^{CG}$ (Zone of Polyphase Foldling and Ductile Shear) Sample 99-14A	$S2^{TZ}$ (Zone of Imbricate Thrust Faults-Caswell Gneiss) Sample 99-35	$S2^{ITZ}$ (Zone of Imbricate Thrust Faults-WFO) Sample 99-35D
1, 2	556_1, 703_2 °C	543_1 °C	601_1 °C	759 °C
3	$T = 644° \pm 86°C$, $P = 8.7 \pm 2.1$ kbar	$T = 551° \pm 22°C$, $P = 6.9 \pm 0.96$ kbar	$T = 813° \pm 132°C$, $P = 7.6 \pm 3.12$ kbar	$T = 794° \pm 148°C$, $P = 7.9 \pm 2.78$ kbar

[a] Thermobarometry methods are (1) garnet-biotite thermometry [*Ferry and Spear*, 1978], (2) garnet-hornblende thermometry [*Graham and Powell*, 1984], and (3) average *P-T* approach of THERMOCALC.

estimates, we used the internally consistent thermodynamic data set of *Holland and Powell* [1990] (data file created April 1996). An explanation of using this method for finding an average *P-T* of the mineral assemblages is presented by *Clarke et al.* [2000]. The results of directly calibrated thermometry and average *P-T* calculations (assuming the activity of water was 1.0 on the basis of hydrous assemblages) are presented in Table 1b. The THERMOCALC barometry results presented in Table 1b become 1–2 kbar lower, and the THERMOCALC thermometry results become 60°–80°C lower if an activity of water of 0.5 is assumed. Errors (2σ) are presented on the average *P* and average *T* calculations. Only rims of minerals (most often in grain contact) were used for the thermobarometry.

[30] Several observations suggest that the conditions of metamorphism we have determined occurred during each of the events we outline. First, the minerals used in calculating *P-T* estimates define the structural elements in the various structural domains. Second, textural relationships suggest syntectonic mineral growth. For example, biotite and muscovite in the schists define mica fish structures consistent with growth during deformation. Third, the relative timing of mineral growth, especially within the Western Fiordland Orthogneiss, is well constrained. Garnet, for example, is only observed in samples intensely deformed within the zone of imbricate thrust faults, indicating syn-$D2^{ITF}$ mineral growth. Finally, only the rims of minerals in grain contact displaying equilibrium textures were probed and used in the determination of pressure and temperature conditions.

[31] Garnet-hornblende and garnet-biotite thermometry for the $S1^{CG}$ assemblage yielded $T = 500°–600°C$ for $P = 4$ kbar. The average *P-T* result suggests that the $S1^{CG}$ assemblage equilibrated at $P = 4.2 \pm 1.88$ kbar and $T = 543° \pm 64°C$, which is consistent with the directly calibrated thermometry. The average *P-T* result for the schists at George Sound (site 99-17; Figure 1b), outside of the zone of diatexite, yielded estimates of $P = 7.6 \pm 1.78$ kbar and $T = 632° \pm 42°C$ which is higher pressures and temperatures than estimated for the $S1^{CG}$ assemblage.

[32] The diatexite assemblages at George Sound from site 97-01 yielded directly calibrated garnet-hornblende and garnet-biotite thermometry estimates of $T = 550°–700°C$ for $P = 8$ kbar (Table 1b). The average *P-T* result suggests that the diatexite assemblage equilibrated at $P = 8.7 \pm 2.1$ kbar and $T = 644° \pm 86°C$ (Table 1b), which is within error of the temperature estimate obtained using directly calibrated thermometry. The average *P-T* result for a second sample of diatexite at George Sound (site 99-13; Figure 1b) yielded estimates of $P = 8.6 \pm 1.52$ kbar and $T = 726° \pm 46°C$.

[33] Garnet-biotite thermometry for the $S2^{CG}$ assemblage (site 99-14; Figure 1b) gives $T = 550°C$ for $P = 8$ kbar. The average *P-T* result suggests that the $S2^{CG}$ assemblage equilibrated at $P = 6.9 \pm 0.96$ kbar and $T = 551° \pm 22°C$, consistent with results from the directly calibrated thermometry. Garnet-biotite thermometry for the high-grade $S2^{ITF}$ assemblages in the Caswell Gneiss and Western Fiordland Orthogneiss (site 99-35; Figure 1b) gives $T = 600°–760°C$ for $P = 8$ kbar. The average *P-T* result suggests that the $S2^{ITF}$ assemblages equilibrated at $P = 7.6 \pm 3.12$ kbar, $T = 813° \pm 132°C$ and $P = 7.9 \pm 2.78$ kbar, $T = 794° \pm 148°C$ for the high-grade Caswell Gneiss and Western Fiordland Orthogneiss samples, respectively.

6.2. Fault Zone Microstructures Inside and Outside the Contact Aureole

[34] In the previous section we showed that mineral assemblages defining the $S2^{CG}$ and $S2^{ITF}$ foliations vary across the structural domains at Caswell Sound. The assemblages and calculated temperatures that accompanied deformation in these zones suggest that the temperature was higher adjacent to the Western Fiordland Orthogneiss. Samples within the Western Fiordland Orthogneiss and up to ~500 m west of its contact yielded results consistent with granulite facies conditions. In contrast, samples within the Caswell Gneiss, deformed by the fold-thrust belt more than 500 m distal to the contact with the Western Fiordland Orthogneiss, give results consistent with amphibolite facies conditions (compare temperatures of 700°–800°C within the contact aureole to estimates of 550°–600°C outside it). In this section, we describe variations in microstructure within the zone of imbricate thrust faults that support our interpretation of a thermal gradient.

[35] To better define the effects of a thermal gradient within the contact aureole, we examined and compared deformation textures in three domains within the zone of imbricate thrust faults: (1) the easternmost thrust zones that cut the Western Fiordland Orthogneiss batholith (e.g., site 99-35; Figure 1b); (2) a thrust zone that deformed the Caswell Gneiss within 100 m of the contact with the Western Fiordland Orthogneiss; and (3) the westernmost imbricate thrust zones that deformed the Caswell Gneiss

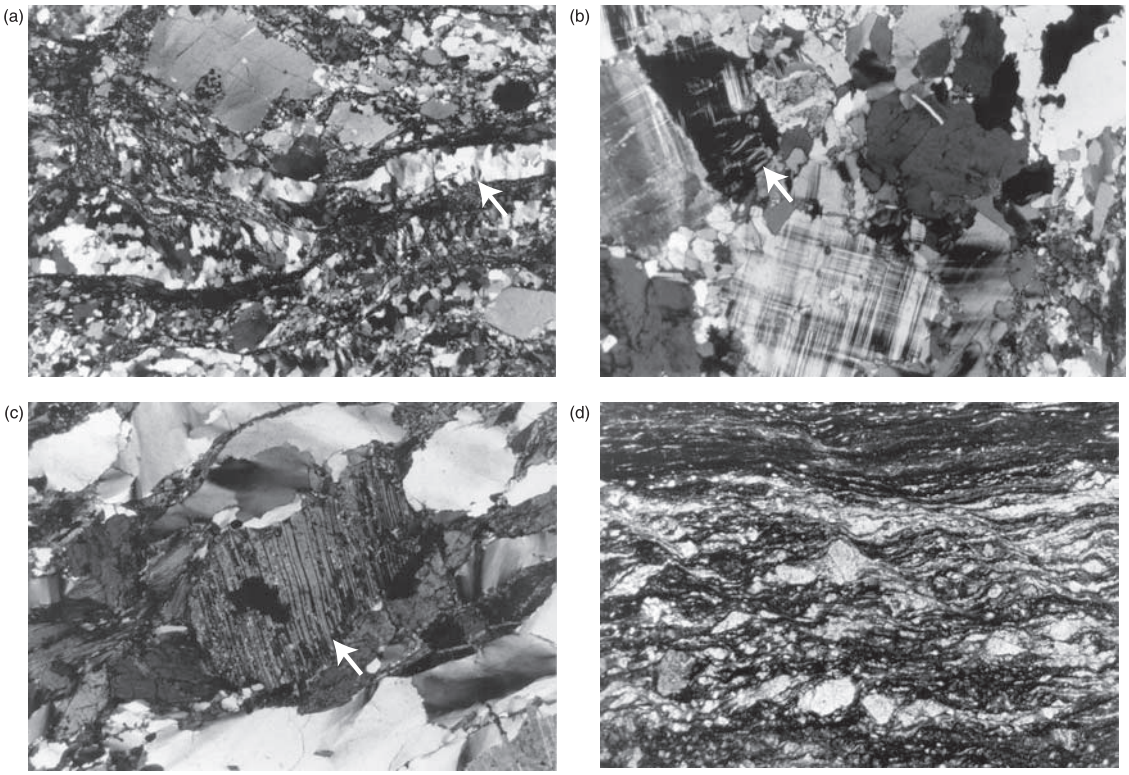

Figure 6. Photomicrographs of mylonite textures in samples from across the Caswell Sound fold-thrust belt. Width of view for each photomicrograph is 3.9 mm. All photomicrographs are taken in crossed polarized light. Figures 6a–6c are samples of Western Fiordland Orthogneiss from site 99-35. Figures 6d–6f are samples of Caswell Gneiss cut by the thrust zone at site 99-29, shown in Figure 6b. (a) Dynamically recrystallized quartz and feldspar. The feldspar porphyroclast at top (arrow) is mantled by recrystallized feldspar. Note boundaries of porphyroclast are serrated. (b) K-feldspar grain with perthitic flames (arrow). (c) Quartz subgrains and bent plagioclase twins (arrow). (d) S-C′ fabric showing top to the right (east) sense of shear. S planes run from left to right, C′ planes run from top left to bottom right. Note zone of ultramylonite at top of photograph. (e) Antithetic microfault in a feldspar porphyroclast. Arrow indicates direction of displacement for the upper side of the fault (i.e., top down to the left (west) sense of shear). (f) Synthetic microfault in a clinozoisite porphyroclast. Arrow points in direction of displacement for the upper side of the fault (i.e., top to the right (east) sense of shear).

2.5 km west of the contact (e.g., site 99-29; Figure 1b). For each domain, samples were collected across the zones and included mylonitic to ultramylonitic samples.

[36] Thrust zones within the Western Fiordland Orthogneiss occur up to a few hundred meters east of its contact with the Caswell Gneiss (Figure 3a). Samples of Western Fiordland Orthogneiss unaffected by thrust zones display a weakly developed foliation defined by amphibole or two-pyroxene assemblages. These samples show limited evidence of deformation during $D2^{ITF}$ such as warped twins in plagioclase grains which otherwise generally display a granoblastic texture. Undulose extinction in quartz and bent twins in plagioclase are common.

[37] Samples of Western Fiordland Orthogneiss from thrust zones contain a well-developed biotite-rich $S2^{ITF}$ foliation with dynamic recrystallization of both feldspar and quartz grains. Large (0.5 mm) quartz grains exhibit strong subgrain development, rotational recrystallization and grain boundary migration. Elongate feldspar grains define the foliation and display core and mantle textures consisting of serrated boundaries surrounded by a mantle of fine recrystallized grains. It is common for the boundary between core and mantle to be blurred or poorly defined (Figure 6a). Feldspar cores show some undulatory extinction, but no fracturing of grains is evident. K-feldspar displays synthetic twinning along the boundaries of inclusions and some grains are microperthitic. Some K-feldspar grains show flame-shaped albite lamellae (Figure 6b) that originate at grain boundaries, typically in pressure shadow positions. Flames are generally widest at the grain boundary and taper to a point within the grain (Figure 6b). These samples also commonly contain narrow bands (<1 mm) of ultramylonite.

[38] Mylonitic to ultramylonitic samples from thrust zones within the Western Fiordland Orthogneiss contain large (0.5 cm) feldspar porphyroclasts displaying undulose extinction that also are mantled by dynamically recrystallized quartz and feldspar grains. The proportion of dynam-

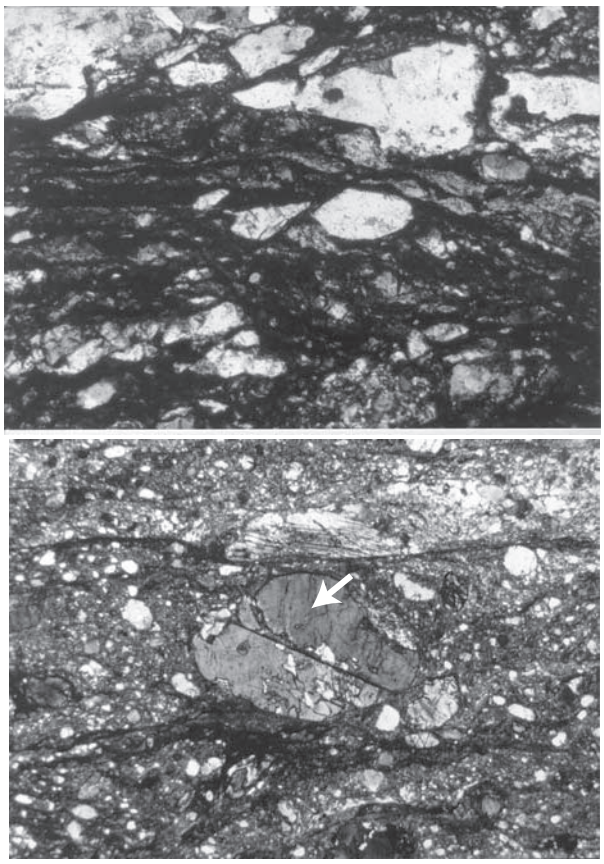

Figure 6. (continued)

ically recrystallized material is much greater in the mylonitic to ultramylonitic samples compared to those described above. Polycrystalline quartz ribbons surround the feldspar porphyroclasts. Many of the quartz ribbons contain elongate single crystals that lack evidence of intracrystalline deformation structures. Ribbons of feldspar are also found in these samples. Feldspar porphyroclasts show well-developed asymmetric tails of recrystallized matrix material. Myrmekite is occasionally found along foliation planes.

[39] Within the Caswell Gneiss samples from thrust zones situated <500 m from the contact show abundant evidence of ductile deformation similar to that described above for the Western Fiordland Orthogneiss. These rocks display evidence of the dynamic recrystallization of feldspar and quartz and recrystallization through the nucleation and growth of new grains at grain boundaries or in segregation bands. These microstructural observations combined with those of *Olsen and Kohlstedt* [1985] and *Pryer* [1993] suggest that the temperatures during deformation in this pluton/contact aureole zone was >550°C.

[40] In contrast, thrust zones more than 500 m from the contact show different textures. For example, samples 2 km west of the Caswell Gneiss/Western Fiordland Orthogneiss contact display little evidence of dynamically recrystallized feldspar. Evidence of subgrain development in quartz includes grains that are mantled by other minor finer-grained dynamically recrystallized quartz grains. Plagioclase porphyroclasts commonly display bent twins, fractures, and undulose extinction (Figure 6c). Twins in plagioclase grains are offset across grain-scale faults and individual twins vary in thickness along their length, most prominently in bent crystals. Elongate and rounded porphyroclasts of clinozoisite, feldspar, and occasionally amphibole are commonly fractured (see, for example, Figures 6d, 6e, and 6f). The fractures usually show little to no displacement and some fractures contain quartz, chlorite, or epidote. Continuous grain fracturing and the separation of broken fragments along the foliation appear to be the principal process resulting in grain size reduction in these samples. Fractured fragments still in contact with one another are angular. A wide range of grain sizes is present in these samples that commonly contain bands of ultramylonite up to 1 mm thick.

[41] East of the westernmost thrust in the imbricate zone (e.g., top of Figure 6d), narrow bands (up to 5 cm thick) of ultramylonitic $S2^{ITF}$ folia that display the same kinematics as the thrust zones are common. Rocks from these areas contain a bimodal grain size with small porphyroclasts of clinozoisite and less commonly feldspar widely dispersed through a very fine-grained matrix of quartz, feldspar, chlorite, and epidote that are elongate in the foliation. Feldspar porphyroclasts show well-developed asymmetric tails of recrystallized matrix material. The long axes of inequant grains have variable orientations relative to the mylonitic foliation and many porphyroclasts have smooth outlines with no obvious mantle. The well-rounded porphyroclasts show very little evidence of internal deformation other than minor fracturing. This characteristic brittle to semi-brittle failure of feldspars in thrust zones more than 500 m from the Western Fiordland Orthogneiss contact coincides with the appearance of chlorite as a main foliation-defining metamorphic mineral. These features, which accompany a change from granulite to amphibolite facies conditions, imply deformation temperatures of <550°C or slightly higher strain rates [*Simpson*, 1985; *Pryer*, 1993]. Temperatures estimated using microstructures indicate relatively cool conditions for development of $S2^{CG}$ outside the imbricate thrust zone and are slightly lower than the 550°–600°C calculated using thermobarometric methods.

[42] In summary, we have found that adjacent to and within the Western Fiordland Orthogneiss, feldspar in thrust zones was dynamically recrystallized, but in thrust zones more than 500 m from the contact, feldspar displayed semi-brittle behavior. The results of microstructural analysis compare reasonably well with our calculated thermometry. However, the thermometric estimates of temperature in the high-grade thrust zones have large errors (2σ error bars on these results were of the order of 100°–150°C), and we think that the results are potentially high ($T = 750°–800°C$). Our microstructural analyses confirm that the temperature of deformation was >550°C. There are four observations that suggest the temperature of deformation was probably <750°–800°C. (1) At temperatures >700°C, we would expect to see evidence of rapid recovery of quartz that would result in strain-free grains as outlined by *Passchier*

and Trouw [1995]. This was not a microstructural feature of the high-grade thrust zones. (2) There was very limited evidence of secondary grain growth in quartz because of grain boundary area reduction as would be expected at temperatures >700°C [*Olsen and Kohlstedt*, 1985]. (3) Flame albite in K-feldspar was common in the Western Fiordland Orthogneiss thrust zones. At temperatures >700°C, this would not be expected [*Pryer*, 1993]. (4) Myrmekite is abundant at temperatures >700°C [*Simpson*, 1985]. We observed only a few small myrmekite grains. For these reasons we feel that 650°–700°C is a more reasonable temperature range for the $D2^{ITF}$ deformation within and near the contact zone of the Western Fiordland Orthogneiss. A second interpretation is that deformation in the thrust zones continued during cooling of the batholith. High-grade metamorphic minerals that grew and equilibrated while the batholith was still very hot may have been preserved during later thrusting when the microstructures we observed developed.

6.3. Relationships Between Deformation and Magmatism

[43] We have shown a clear link between metamorphic conditions, feldspar microstructure, and proximity to the Western Fiordland Orthogneiss during $D2^{ITF}$ deformation. We suggest that because the Western Fiordland Orthogneiss and the adjacent country rock were still relatively hot (650°–700°C or possibly higher) at the time of deformation, imbricate thrust faulting must have followed shortly after emplacement of the batholith in the Caswell Sound region. This is supported by the similar conditions preserved in the George Sound diatexites and the imbricate thrust zone at Caswell Sound. Pressure estimates of P = 7–9 kbar from the imbricate thrust zone indicate a depth of approximately 25–30 km for thrust faulting in the Caswell Sound region. Metamorphic data from the George Sound (P = 7–9 kbar) diatexites suggest an emplacement depth of ~25–30 km for the Western Fiordland Orthogneiss batholith.

7. Sense of Shear Indicators

[44] In this section we describe microstructural and macroscopic indicators used to determine the senses of displacement during formation of the Caswell fold-thrust belt. Boudinaged grains and layering show that the $L2^{CG}$ and $L2^{ITF}$ mineral lineations are true stretching directions. In our analysis, we compare microstructures and lineation directions in the zone of imbricate thrust faults with those in the zone of polyphase folding and ductile shear.

[45] Fault propagation folds occur at the termination points of many ultramylonitic thrust ramps (e.g., Figure 3b). These structures indicate west up over east senses of displacement (or Caswell Gneiss over Western Fiordland Orthogneiss). Other macroscopic indicators of sense of displacement include ~0.5 m wide recumbent overfolds of sedimentary or igneous layers with inverted limbs that are often sheared out by minor thrust zones displaying west up over east offsets (Figure 4c). In the high-grade thrust zones within and proximal to the Western Fiordland Orthogneiss, shear zone cleavages (C′ cleavage and S-C fabric in Figure 6d), and >90% of asymmetric tails on feldspar augen and asymmetric mica fish indicate west up over east sense of shear. Distal to the Western Fiordland Orthogneiss, antithetic (Figure 6b) and synthetic (Figure 6c) microfaults in feldspar grains and asymmetric quartz microstructures (e.g., oblique shape-preferred foliation) also indicate west up over east in the imbricate thrust zone. Surfaces oriented parallel to the $L2^{ITF}$ lineations and perpendicular to $S2^{ITF}$ foliation planes record the maximum amount of asymmetry indicating that the lineations coincide with the direction of tectonic transport. The consistency of kinematic indicators and lineation directions within the zone of imbricate thrust zones also suggest that these structures are reliable indicators of displacement sense and direction, respectively.

[46] $L2^{CG}$ lineation measurements in the zone of polyphase folding and ductile shear plunge gently to the south and south-southeast at high angles (~60°–90°) to $L2^{ITF}$ in the zone of imbricate thrust faults. However, unlike the zone of imbricate thrusts, asymmetric structures and well-developed sense of shear indicators do not occur within the zone of polyphase folding and ductile shear. In the narrow west vergent thrust domain asymmetric structures record east over west displacements parallel to a moderately east plunging stretching lineation. If $D2^{CG}$ and $D2^{ITF}$ deformation were simultaneous or progressive across the fold-thrust belt, then the differences in $L2^{CG}$ and $L2^{ITF}$ lineation orientations indicate that north-south stretching in the zone of polyphase folding and ductile shear occurred during east directed thrust transport in the zone of imbricate thrust faults.

8. Kinematic Model of Fold-Thrust Belt Evolution

[47] The two-sided geometry of the Caswell fold-thrust belt defined by the opposing orientations of west vergent thrusts and east vergent imbricate thrusts suggests that these thrust zones resulted from subhorizontal (east-west) compression and may represent conjugate structures. The kinematics, structural style, and metamorphic assemblages within the two sets of thrusts are consistent with them representing conjugates. Figure 7a represents an interpretation of structures and intrusions as they may have looked prior to the development of the Caswell fold-thrust belt and shortly after emplacement of the Western Fiordland Orthogneiss. Our analyses indicate that rheologically weak zones preferentially localized contractional deformation into thrust planes. This latter result is supported by the preferential occurrence of thrust zones in the marble layers of the Caswell Gneiss, in the zone of thermally weakened crust in the Western Fiordland Orthogneiss aureole, and between the marbles and the undeformed McKerr monzodiorite in the west vergent thrust zone (Figure 7b). The geometry of upright $F2^{CG}$ folds and the steep orientation of $S2^{CG}$ in the zone of open folding also are consistent with east-west shortening and subhorizontal compression.

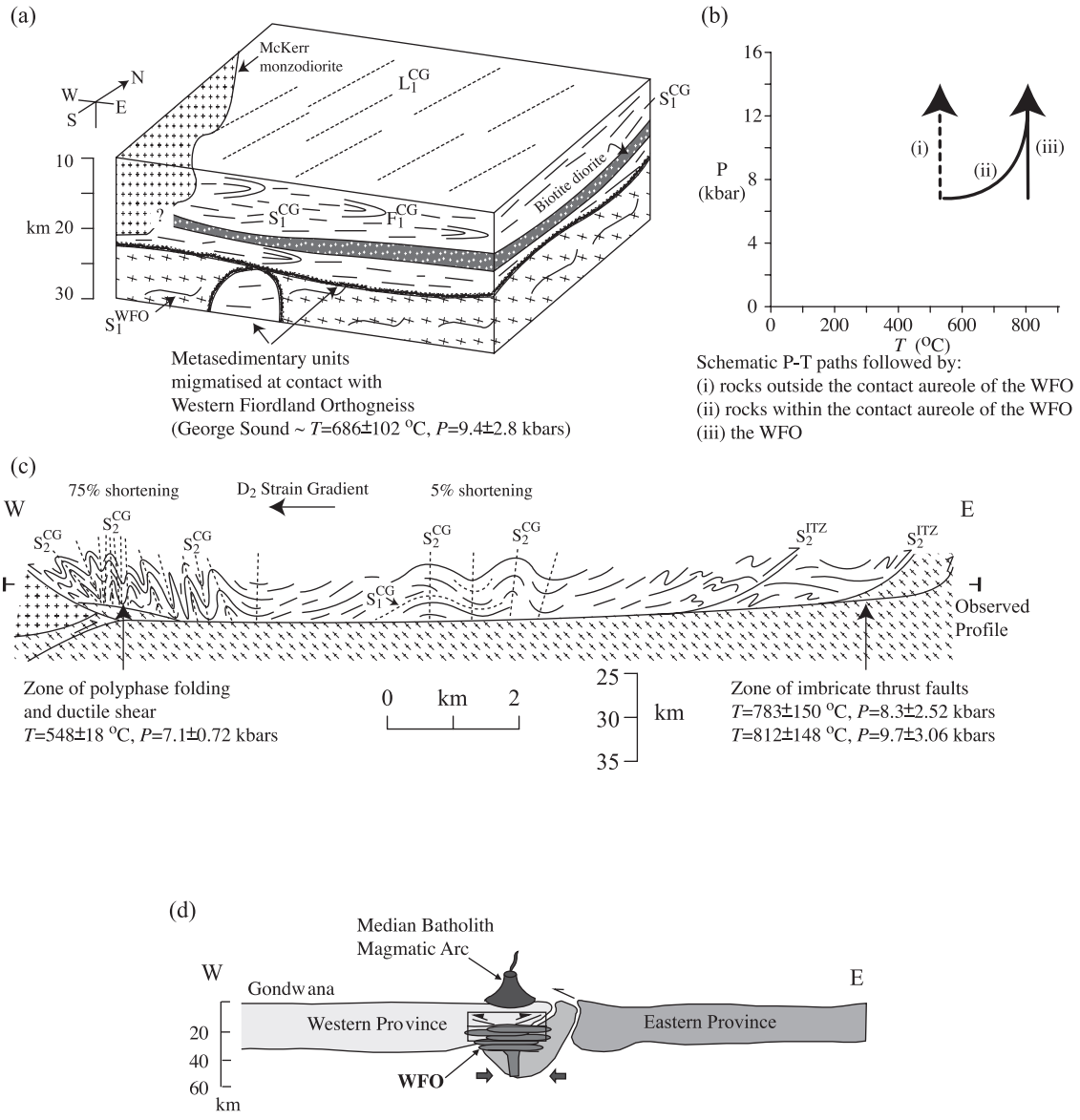

Figure 7. (a) Summary diagram of the intrusive relationships of the Western Fiordland Orthogneiss batholith prior to development of the Caswell fold-thrust belt. The Western Fiordland Orthogneiss is inferred to have been emplaced as a series of shallowly dipping sills that most commonly have shallowly dipping contacts with the country rocks [*Bradshaw*, 1990]. The lines labeled S_1^{WFO} represent a shallowly dipping foliation (possible of magmatic origin) within the Western Fiordland Orthogneiss. The metasedimentary units are migmatized within the contact aureole of the Western Fiordland Orthogneiss. (b) *P-T* path followed by the Western Fiordland Orthogneiss and adjacent country rock. The Western Fiordland Orthogneiss was loaded soon after emplacement and therefore would have followed the vertical full line shown in *P-T* space. The Paleozoic country rocks were much cooler and would have been loaded to similar depths and heated slightly. There was probably not enough time for them to heat substantially [*Bradshaw*, 1989a]. The Paleozoic country rocks within the aureole would have heated up before or during loading (curved full line). (c) Interpretative cross section of the Caswell fold-thrust belt showing basal décollement at the roof of the Western Fiordland Orthogneiss. (d) Regional section across the Median Batholith and Eastern and Western Provinces of New Zealand showing the relative position (box) of the Caswell fold-thrust belt at the root of the Early Cretaceous magmatic arc. Note two-sided thrust belt at top of the Western Fiordland Orthogneiss (WFO). Evidence of convergence below the fold-thrust belt is from *Daczko et al.* [2001a].

[48] In the zone of open folding the subhorizontal $S1^{CG}$-$L1^{CG}$ fabric forms the dominant structure. Thrust surfaces are absent in this zone, and $F2^{CG}$ folds are broad open warps of $S1^{CG}$. $S2^{CG}$ is widely spaced and weakly developed and recrystallization of the $S1^{CG}$-$L1^{CG}$ fabric is minimal. These observations suggest that the zone of open folding is an area of low $D2^{CG}$ strain. We have confirmed this interpretation using the simple method of measuring the final versus initial lengths of folded $S1^{CG}$ surfaces in parts of this zone to estimate the amount of $D2^{CG}$ shortening parallel to the dominant transport direction of the fold-thrust belt. These measurements may vary with different folding mechanisms but suggest that as little as 5% shortening by $F2^{CG}$ folding occurred in most parts of the zone of upright folding.

[49] In the zones of polyphase folding and imbricate thrusts $F2^{CG}$ folds are tight to isoclinal and minor thrust zones shear out $F2^{CG}$ fold limbs. Linear strain measurements using folded foliation surfaces suggest that as much as ~75% shortening by $F2^{CG}$ folding occurred during $D2^{CG}$ deformation in these two areas. In accordance with the estimates of linear strains, the $S2^{CG}$ foliation in these areas is intensely developed and commonly transposes the older $S1^{CG}$ foliation. These observations confirm that the zones of polyphase folding and imbricate thrust faults are areas of high $D2^{CG}/D2^{ITF}$ strain. East of the imbricate thrust zone and west of the west vergent thrust zone, the effects of contractional deformation are minimal to nil (Figure 2c).

[50] We have shown that strain is localized at the contact between the Western Fiordland Orthogneiss and Caswell Gneiss. This information combined with the listric geometry of the imbricate thrusts suggests that a buried décollement surface should occur at depth (Figure 7b). The Western Fiordland Orthogneiss outcrops to the north and south of Caswell Sound (George Sound and Charles Sound, respectively; Figure 1), and hence this unit is inferred to be below the exposed level of the Caswell Gneiss and Caswell fold-thrust belt at Caswell Sound. The geometry of open folding, the lack of thrust zones, and the small degree of shortening (~5%) in the zone of upright folding located structurally above the Western Fiordland Orthogneiss contact also suggest that the Caswell Gneiss is detached from the Western Fiordland Orthogneiss. The original intrusive geometry of the Western Fiordland Orthogneiss may also have controlled the geometry of the cross section shown in Figure 7b. For example, *Bradshaw* [1990] interprets the Western Fiordland Orthogneiss as having been emplaced as a series of shallowly dipping sills and this geometry would have been more favorable to the development of a buried décollement surface at depth compared with an original steep walled geometry to the Western Fiordland Orthogneiss.

[51] Strain localization in the zone of polyphase folding and ductile shear and the formation of west vergent thrusts that separate highly deformed marbles and schists from the undeformed McKerr monzodiorite strongly suggests the presence of a buried thrust ramp. Similar geometries of conjugate thrusts or backthrusts located above buried ramps involving crystalline thrust sheets are well documented in fold-thrust belts in other convergent settings [e.g., *Klepeis*, 1994, Figure 3b; *McClay and Buchanan*, 1992; *Merle*, 1998, Figure 61]. Delamination of the section along weak marble horizons between two converging, strong blocks represented by the undeformed, unmetamorphosed McKerr monzodiorite and the crystalline Western Fiordland Orthogneiss can explain the observed geometry (Figure 7b). The inferred existence of this buried thrust ramp is consistent with our observations that thrusts in the imbricate zone involve the Western Fiordland Orthogneiss. We also suggest that the localized north-south stretching in this zone resulted from the ductile extrusion and subsequent spreading of weak, ductilely deforming paragneisses and marbles between these two converging rigid blocks. The observed patterns resemble other zones of ductile extrusion between crystalline thrust sheets such as the Morcles nappe in the Helvetic Alps [*Merle*, 1989; *Ratschbacher et al.*, 1991].

9. Discussion

[52] In this section we discuss our results in context with published models of the development of the Fiordland high-pressure granulites. We also evaluate the significance of our research for interpreting processes affecting the deep levels of magmatic arcs.

[53] On the basis of regional correlations and geochronological work completed south of Caswell Sound [e.g., *Ireland and Gibson*, 1998] the fabric we have labeled $S1^{CG}$ is most likely Paleozoic in age. The age of $S1^{WFO}$, however, must be Early Cretaceous on the basis of well-documented 126–116 Ma ages from the Western Fiordland Orthogneiss [*Mattinson et al.*, 1986; *Gibson et al.*, 1988; *Gibson and Ireland*, 1995; *Muir et al.*, 1998]. Hence $S1^{CG}$ and $S1^{WFO}$ are unrelated. Both these foliations are overprinted by D2 deformation and all thrust zones of the Caswell fold-thrust belt, indicating an Early Cretaceous age for the development of the fold-thrust belt.

[54] Metamorphic assemblages within the contact aureole between Paleozoic country rock and the Western Fiordland Orthogneiss at George and Caswell Sounds indicate an emplacement depth of ~25–30 km (P = 7–9 kbar) for the pluton. The contact at Caswell Sound is deformed by a series of imbricate east vergent thrust zones that formed under high-grade (granulite and amphibolite facies) metamorphic conditions and form part of an ~2-km-wide, two-sided fold-thrust belt (Figures 2 and 7). The Western Fiordland Orthogneiss is cut by garnet granulite reaction zones in which enstatite and hornblende are mantled by garnet-clinopyroxene-bearing assemblages that reflect ~25 km of Early Cretaceous burial [*Bradshaw*, 1989a; *Clarke et al.*, 2000; *Daczko et al.*, 2001b]. These structural relationships and metamorphic assemblages within and adjacent to the pluton imply that the Western Fiordland Orthogneiss underwent tectonic loading by the imbrication of thrust sheets following middle to deep crustal emplacement of the pluton in the Early Cretaceous. This contractional style of deformation and loading predate the onset of extension at ~108 Ma (age of extension from Tulloch and Kimbrough [1989]).

[55] Three models have been proposed previously to explain the origin of the high-pressure granulite facies conditions in Fiordland. First, *Gibson et al.* [1988] and

Gibson and Ireland [1995] suggested that the Western Fiordland Orthogneiss intruded into the lower crust (at $P >$ 12 kbar) within a divergent tectonic regime. They inferred that ductile normal faulting subsequently tectonically exhumed the Western Fiordland Orthogneiss during the mid-Cretaceous (~105 Ma). Second, *Mattinson et al.* [1986], *Bradshaw* [1989a], and *Bradshaw and Kimbrough* [1989] hypothesized a middle to deep crustal ($P = 6–7$ kbar) emplacement depth for the Western Fiordland Orthogneiss and used tectonic loading by overthrusts to explain a Cretaceous up-pressure history recorded in western Fiordland. They observed metamorphic assemblages interpreted to represent $P = 6–7$ kbar that were overprinted by high-pressure assemblages at $P = 12–13$ kbar in the Paleozoic paragneiss. Jadeite zoning patterns in clinopyroxene and garnet-clinopyroxene granulite assemblages that cut two-pyroxene hornblende granulite facies assemblages in the Western Fiordland Orthogneiss also supported their model. Finally, *Oliver* [1990] and *Brown* [1996] proposed a model involving magma loading to explain the observations made by *Bradshaw* [1989a]. This model was attractive because at that time no thrust sheets had been discovered in western Fiordland to support tectonic loading by overthrusts. SHRIMP dating of monazite in Paleozoic paragneiss at Doubtful Sound suggested a Paleozoic age of the assemblages used by *Bradshaw* [1989a] to infer a Cretaceous up-pressure metamorphic history [*Ireland and Gibson*, 1998], throwing doubt on models involving Cretaceous loading. However, *Clarke et al.* [2000] used thermodynamic modeling of Cretaceous metamorphic assemblage changes in the Arthur River Complex and Western Fiordland Orthogneiss in northern Fiordland (Figure 1) to confirm a Cretaceous up-pressure loading of these rocks. *Daczko et al.* [2001a] presented quantitative kinematic analyses that indicated intense lower crustal ($P = 14$ kbar) contraction within a pure shear dominated flow regime and ductile thrust faulting that followed the Cretaceous loading history reported by *Clarke et al.* [2000]. This deformation occurred at depths of >45 km and possibly represents contractional orogenesis in the deepest crust that followed the development of the Caswell fold-thrust belt at midcrustal levels. Nevertheless, the data presented by *Daczko et al.* [2001a], like those we present here from Caswell Sound, indicate that shortening dominated the postemplacement history of the batholith in western Fiordland (Figures 7c and 7d).

[56] This paper presents the first evidence from western Fiordland that a fold-thrust belt style of contractional deformation deformed the upper contact of the Early Cretaceous Western Fiordland Orthogneiss. This result supports an interpretation of the tectonic loading of both the Western Fiordland Orthogneiss and its country rocks to explain the up-pressure history recorded by metamorphic assemblages. However, we point out that this result does not exclude a component of magma loading during emplacement of the Fiordland high-pressure granulite facies belt. Nevertheless, it does indicate that a compressional tectonic regime accompanied and outlasted emplacement of the voluminous Western Fiordland Orthogneiss [cf. *Gibson et al.*, 1988; *Gibson and Ireland*, 1995; *Ireland and Gibson*, 1998].

[57] Studies of other magmatic belts in North America, South America, and elsewhere have shown that the thickness of arc crust generally increases through time [*Coward et al.*, 1986; *Brown and Walker*, 1993; *Tobisch et al.*, 1995; *Crawford et al.*, 1999; *Miller et al.*, 2000]. One question that is relevant to all arc systems is how this thickening occurs and whether large contractional faults are involved in the process. For example, in the northern Cascades of the northwest United States, an up-pressure metamorphic history is recorded in changing metamorphic mineral assemblages at the roots of a Cretaceous arc, but the driving force of burial and whether it involved thrust faulting, magmatic loading, pure shear thickening, or some other mechanism is controversial (see *Miller et al.* [2000] for a review). In the central Coast Mountains Batholith of northern British Columbia and southeast Alaska, a midcrustal contractional history is implied by regional relationships and the kinematics of penetrative ductile fabrics [*Klepeis et al.*, 1998; *Crawford et al.*, 1999]. However, evidence of discrete thrust zones and the effects of possible thrusting on the mechanical and thermal evolution of this arc mostly has been obliterated by the formation of migmatites, pluton emplacement, and postcontractional ductile normal faulting. The Fiordland data are important to the study of magmatic arcs because they indicate that loading via the imbrication of thrust sheets in the deep crust is a viable mechanism for the crustal thickening observed in arc environments. These relationships also provide direct evidence that thrust loading contributed to the characteristic up-pressure pattern of metamorphism which has been observed in other magmatic belts in different settings [e.g., *Brown and Walker*, 1993; *Paterson and Miller*, 1998; *Whitney et al.*, 1999].

[58] Some studies of magmatic belts also suggest that pluton emplacement mechanisms and processes controlling the evolution of arc crust vary with depth. For example, *Miller and Paterson* [1999] proposed that plutons in some parts of the northern Cascades representative of upper crust ascended as viscoelastic diapirs enclosed by host rocks that were deforming by both ductile and brittle processes. Buoyancy rather than regional stress was inferred to control the ascent of magma in this setting. In contrast, studies of deep crustal exposures have shown that displacements along ductile faults also can control the emplacement of sheet-like intrusive bodies [*Klepeis and Crawford*, 1999; *Crawford et al.*, 1999]. The Fiordland data support interpretations that large vertical displacements at the deepest levels of magmatic arcs may commonly involve tectonic imbrication and the development of discrete thrust zones.

[59] Finally, we suggest that the partitioning of thrust zones into thermally softened crust at Caswell Sound suggests that the emplacement geometry and orientation of the contacts of the Western Fiordland Orthogneiss influenced the style of contractional deformation affecting the batholith. At Caswell Sound, thrust zones reactivated the gently dipping Western Fiordland Orthogneiss/country rock contact and the gently dipping $S1^{CG}$ layering in country rocks. In contrast, the steep-walled geometry of the Western Fiordland Orthogneiss contact at George Sound appears to have shielded the contact at that locality from developing

fold-thrust belt geometries. These data support interpretations of deformation patterns in other crustal sections [e.g., *Miller and Paterson*, 2001] by suggesting that mechanical anisotropies created by inherited compositional layering influenced the style of contractional deformation in the deep crustal portions of the batholith in Fiordland.

10. Conclusions

[60] Structural and metamorphic data from the middle-lower crustal roots of a composite batholith in western Fiordland show that loading by the imbrication of thrust sheets in the deep crust is a viable mechanism for the crustal thickening in arc environments. We document imbricate, granulite facies to amphibolite facies thrust zones that form part of a newly discovered middle-lower crustal (25–30 km) fold-thrust belt that cuts the uppermost contact of the Early Cretaceous (126–116 Ma) Western Fiordland Orthogneiss. Our data indicate that contraction outlasted emplacement of the Western Fiordland Orthogneiss and controlled the tectonic evolution of the batholith. Thrust faulting produced mylonitic to ultramylonitic fabrics in a well-defined ~3-km-wide zone of imbricate thrust faults that formed within and at the margin of the Western Fiordland Orthogneiss. These thrust zones contain high-grade garnet-biotite-K-feldspar granulite facies assemblages within 500 m of the contact and chlorite-epidote amphibolite facies assemblages further from the Western Fiordland Orthogneiss contact. The localization of high-grade mylonitic to ultramylonitic thrust zones at and near the Western Fiordland Orthogneiss contact implies that thrust zones were preferentially partitioned into crust that was thermally weakened by magmatism. Our results show that large vertical displacements within an Early Cretaceous magmatic arc were linked to thrust imbrication in the deep crust and produced an up-pressure metamorphic history that is similar to that observed in other magmatic belts worldwide.

[61] **Acknowledgments.** Funding to support this work was provided by two University of Sydney Institutional Australian Research Council grants to K. A. Klepeis; a large Australian Research Council grant to K. A. Klepeis and G. L. Clarke (A10009053), and a National Science Foundation (EAR-0087323) grant to K. A. Klepeis and T. Rushmer. An Australian postgraduate award from the University of Sydney supported N. R. Daczko during preparation of this manuscript. We are especially grateful to Nick Mortimer and Andy Tulloch of the IGNS, Dunedin for many helpful discussions and logistical assistance, and to the Department of Conservation in Te Anau for permission to visit and sample localities in the Fiordland National Park. We also thank N. M. Kelly for assistance in the field and laboratory and Gabriela Mora-Klepeis for many helpful discussions.

References

Andronicos, C. L., L. S. Hollister, C. Davidson, and D. Chardon, Kinematics and tectonic significance of transpressive structures within the Coast Plutonic Complex, British Columbia, *J. Struct. Geol.*, *21*, 229–243, 1999.

Bishop, D. G., J. D. Bradshaw, and C. A. Landis, Provisional terrain map of South Island, New Zealand, in *Tectonostratigraphic Terranes of the Circum-Pacific Region*, edited by D. G. Howell et al., pp. 512–522, Circum-Pacific Counc. for Energy and Resour., Houston, Tex., 1985.

Blattner, P., The North Fiordland transcurrent convergence, *N. Z. J. Geol. Geophys.*, *34*, 543–553, 1991.

Bradshaw, J. D., Cretaceous geotectonic patterns in the New Zealand region, *Tectonics*, *8*, 803–820, 1989.

Bradshaw, J. D., A review of the Median Tectonic Zone: Terrane boundaries and terrane amalgamation near the Median Tectonic Line, *N. Z. J. Geol. Geophys.*, *36*, 117–125, 1993.

Bradshaw, J. Y., and D. L. Kimbrough, Comment: Age constraints on metamorphism and the development of a metamorphic core complex in Fiordland, southern New Zealand, *Geology*, *17*, 380–381, 1989.

Bradshaw, J. Y., Origin and metamorphic history of an Early Cretaceous polybaric granulite terrain, Fiordland, southwest New Zealand, *Contrib. Mineral. Petrol.*, *103*, 346–360, 1989a.

Bradshaw, J. Y., Early Cretaceous vein-related garnet granulite in Fiordland, southwest New Zealand: A case for infiltration of mantle-derived CO_2-rich fluids, *J. Geol.*, *97*, 697–717, 1989b.

Bradshaw, J. Y., Geology of crystalline rocks of northern Fiordland: Details of the granulite facies Western Fiordland Orthogneiss and associated rock units, *N. Z. J. Geol. Geophys.*, *33*, 465–484, 1990.

Brown, E. H., High-pressure metamorphism caused by magma loading in Fiordland, New Zealand, *J. Metamorph. Geol.*, *14*, 441–452, 1996.

Brown, E. H., and N. W. Walker, A magma-loading model for Barrovian metamorphism in the southeast Coast Plutonic Complex, British Columbia and Washington, *Geol. Soc. Am.. Bull.*, *105*, 479–500, 1993.

Carter, R. M., C. A. Landis, R. J. Norris, and D .G. Bishop, Suggestions towards a high-level nomenclature for New Zealand rocks, *J. R. Soc. N. Z.*, *4*, 29–84, 1974.

Clarke, G. L., K. A. Klepeis, and N. R. Daczko, Cretaceous high-P granulites at Milford Sound, New Zealand: Their metamorphic history and emplacement in a convergent margin setting, *J. Metamorph. Geol.*, *18*, 359–374, 2000.

Coward, M. P., B. F. Windley, R. D. Broughton, I. W. Luff, M. G. Petterson, C. J. Pudsey, D. C. Rex, and M. Asif Khan, Collision tectonics in the northwest Himalayas, in *Collision Tectonics*, edited by M. P. Coward and A. C. Ries, *Geol. Soc. Spec. Publ., 19*, 203–219, 1986.

Crawford, M. L., K. A. Klepeis, G. Gehrels, and C. Isachsen, Batholith emplacement at mid-crustal levels and its exhumation within an obliquely convergent margin, *Tectonophysics*, *312*, 57–78, 1999.

Daczko, N. R., K. A. Klepeis, and G. L. Clarke, Evidence of Early Cretaceous collisional-style orogenesis in northern Fiordland, New Zealand and its effects on the evolution of the lower crust, *J. Struct. Geol.*, *23*, 693–713, 2001a.

Daczko, N. R., G. L. Clarke, and K. A. Klepeis, Transformation of two-pyroxene hornblende granulite to garnet granulite involving simultaneous melting and fracturing of the lower crust, Fiordland, New Zealand, *J. Metamorph. Geol.*, *19*, 549–562, 2001b.

Ferry, J. M., and F. S. Spear, Experimental calibration of the partitioning of Fe and Mg between biotite and garnet, *Contrib. Mineral. Petrol.*, *66*, 113–117, 1978.

Gibson, G. M., and T. R. Ireland, Granulite formation during continental extension in Fiordland, *Nature*, *375*, 479–482, 1995.

Gibson, G. M., and T. R. Ireland, Extension of Delamarian (Ross) orogen into western New Zealand: Evidence from zircon ages and implications for crustal growth along the Pacific margin of Gondwana, *Geology*, *24*, 1087–1090, 1996.

Gibson, G. M., I. McDougall, and T. R. Ireland, Age constraints on metamorphism and the development of a metamorphic core complex in Fiordland, southern New Zealand, *Geology*, *16*, 405–408, 1988.

Graham, C. M., and R. Powell, A garnet-hornblende geothermometer: Calibration, testing, and application to the Pelona Schist, southern California, *J. Metamorph. Geol.*, *2*, 13–31, 1984.

Grocott, J., M. Brown, R. D. Dallmeyer, G. K. Taylor, and P. J. Treloar, Mechanism of continental growth in extensional arcs: An example from the Andean plate boundary zone, *Geology*, *22*, 91–394, 1994.

Hill, E. J., A deep crustal shear zone exposed in western Fiordland, New Zealand, *Tectonics*, *14*, 1172–1181, 1995a.

Hill, E. J., The Anita Shear Zone: A major, middle Cretaceous tectonic boundary in northwestern Fiordland, *N. Z. J. Geol. Geophys.*, *38*, 93–103, 1995b.

Hodges, K. V., and F. S. Spear, Geothermometry, geobarometry and the Al2SiO5 triple point at Mt. Moosilauke, New Hampshire, *Am. Mineral.*, *66*, 1118–1134, 1982.

Holland, T. J. B., and R. Powell, An enlarged and updated internally consistent thermodynamic data set with uncertainties and correlations: The system K_2O-Na_2O-CaO-MgO-MnO-FeO-Fe_2O_3-Al_2O_3-TiO_2-SiO_2-C-H_2O-O_2, *J. Metamorph. Geol.*, *8*, 89–124, 1990.

Ingram, G. M., and D. H. W. Hutton, The Great Tonalite sill: Emplacement into a contractional shear zone and implications for Late Cretaceous to early

Eocene tectonics in southeastern Alaska and British Columbia, *Geol. Soc. of Am. Bull.*, *106*, 715–728, 1994.

Ireland, T. R., and G. M. Gibson, SHRIMP monazite and zircon geochronology of high-grade metamorphism in New Zealand, *J. Metamorph. Geol.*, *16*, 149–167, 1998.

Kimbrough, D. L., A. J. Tulloch, E. Geary, D. S. Coombs, and C. A. Landis, Isotope ages from the Nelson region of South Island, New Zealand: Structure and definition of the Median Tectonic Zone, *Tectonophysics*, *225*, 433–448, 1993.

Kimbrough, D. L., A. J. Tulloch, D. S. Coombs, C. A. Landis, M. R. Johnston, and J. L. Mattinson, Uranium-lead zircon ages from the Median Tectonic Zone, New Zealand, *N. Z. J. Geol. Geophys.*, *37*, 393–419, 1994.

Klepeis, K., Relationship between uplift of the metamorphic core of the southernmost Andes and shortening in the Magallanes foreland fold and thrust belt, Tierra Del Fuego, Chile, *Tectonics*, *13*, 882–904, 1994.

Klepeis, K. A., and M. L. Crawford, High-temperature arc-parallel normal faulting and transtension at the roots of an obliquely convergent orogen, *Geology*, *27*, 7–10, 1999.

Klepeis, K. A., M. L. Crawford, and G. Gehrels, Structural history of the crustal-scale Coast shear zone near Portland Canal, Coast Mountains orogen, southeast Alaska and British Columbia, *J. Struct. Geol.*, *20*, 883–904, 1998.

Klepeis, K. A., N. R. Daczko, and G. L. Clarke, Kinematic vorticity and the tectonic significance of superposed mylonites in a major lower crustal shear zone, northern Fiordland, New Zealand, *J. Struct. Geol.*, *21*, 1385–1405, 1999.

Landis, C. A., and D. S. Coombs, Metamorphic belts and orogenesis in southern New Zealand, *Tectonophysics*, *4*, 501–518, 1967.

MacKinnon, T. C., Origin of the Torlesse terrane and coeval rocks, South Island, New Zealand, *Geol. Soc. Am. Bull.*, *94*, 967–985, 1983.

Mattinson, J. L., D. L. Kimbrough, and J. Y. Bradshaw, Western Fiordland orthogneiss: Early Cretaceous arc magmatism and granulite facies metamorphism, New Zealand, *Contrib. Mineral. Petrol.*, *92*, 383–392, 1986.

McClay, K. R., and P. G. Buchanan, Thrust faults in inverted extensional basins, in *Thrust Tectonics*, edited by K. R. McClay, pp. 93–104, Chapman and Hall, New York, 1992.

Merle, O., Strain patterns within spreading nappes, *Tectonophysics*, *165*, 57–71, 1989.

Merle, O., *Emplacement Mechanisms of Nappes and Thrust Sheets*, 159 pp., Kluwer Acad., Norwell, Mass., 1998.

Miller, R. B., and S. R. Paterson, In defense of magmatic diapirs, *J. Struct. Geol.*, *21*, 1161–1173, 1999.

Miller, R. B., and S. R. Paterson, Influence of lithological heterogeneity, mechanical anisotropy, and magmatism on the rheology of an arc, North Cascades, Washington, *Tectonophysics*, *342*, 351–370, 2001.

Miller, R. B., E. H. Brown, D. P. McShane, and D. L. Whitney, Intra-arc crustal loading and its tectonic implications, North Cascades crystalline core, Washington and British Colombia, *Geology*, *21*, 255–258, 1993.

Miller, R. B., S. R. Paterson, S. M. DeBari, and D. L. Whitney, North Cascades Cretaceous crustal section: Changing kinematics, rheology, metamorphism, pluton emplacement and petrogenesis from 0 to 40 km depth, in *Guidebook for Geological Field Trips in Southwestern British Columbia and Northern Washington*, edited by G. L. Woodsworth et al., pp. 229–278, Geol. Assoc. of Can., Cordilleran Sect., St. John's, NF, Canada, 2000.

Mortimer, N., Triassic to Early Cretaceous tectonic evolution of New Zealand terranes: A summary of recent data and an integrated model, in *Proceedings of the 1995 PACRIM Congress, Australasian Institute of Mining and Metallurgy, Carlton, Victoria, Australia*, edited by J. L. Mauk and J. D. St. George, pp. 401–406, Australas. Inst. of Min. and Metal., Parkville, Vic., Australia, 1995.

Mortimer, N., A. J. Tulloch, R. N. Spark, N. W. Walker, E. Ladley, A. Allibone, and D. L. Kimbrough, Overview of the Median Batholith, New Zealand: A new interpretation of the geology of the Median Tectonic Zone and adjacent rocks, *J. Afr. Earth Sci.*, *29*, 257–268, 1999.

Muir, R. J., S. D. Weaver, J. D. Bradshaw, G. N. Eby, and J. A. Evans, The Cretaceous Separation Point batholith, New Zealand: Granitoid magmas formed by melting of a mafic lithosphere, *J. Geol. Soc. London*, *152*, 689–701, 1995.

Muir, R. J., S. D. Weaver, J. D. Bradshaw, G. N. Eby, J. A. Evans, and T. R. Ireland, Geochemistry of the Karamea Batholith, New Zealand, and comparisons with the Lachlan Fold Belt granites of SE Australia, *Lithos*, *39*, 1–20, 1996.

Muir, R. J., T. R. Ireland, S. D. Weaver, J. D. Bradshaw, J. A. Evans, G. N. Eby, and D. Shelly, Geochronology and geochemistry of a Mesozoic magmatic arc system, Fiordland, New Zealand, *J. Geol. Soc. London*, *155*, 1037–1053, 1998.

Oliver, G. J. H., An exposed cross-section of continental crust, Doubtful Sound Fiordland, New Zealand: Geophysical and geological setting, in *Exposed Cross–Sections of the Continental Crust*, edited by M. H. Fountain and D. M. Salisbury, pp. 43–69, Kluwer Acad., Norwell, Mass., 1990.

Oliver, G. J. H., and J. H. Coggon, Crustal structure of Fiordland, New Zealand, *Tectonophysics*, *54*, 253–292, 1979.

Olsen, T. S., and D. L. Kohlstedt, Natural deformation and recrystallisation of some intermediate plagioclase feldspars, *Tectonophysics*, *111*, 107–131, 1985.

Passchier, C. W., and R. A. J. Trouw, *Microtectonics*, Springer-Verlag, New York, 1995.

Paterson, S. R., and R. B. Miller, Magma emplacement during arc-perpendicular shortening: An example from the Cascades crystalline core, Washington, *Tectonics*, *17*, 571–586, 1998.

Powell, R., and T. J. B. Holland, An internally consistent data set with uncertainties and correlations, 3, Applications to geobarometry, worked examples and a computer program, *J. Metamorph. Geol.*, *6*, 173–204, 1988.

Pryer, L. L., Microstructures in feldspars from a major crustal thrust zone: The Grenville Front, Ontario, Canada, *J. Struct. Geol.*, *15*, 21–36, 1993.

Ratschbacher, L., H. R. Wenk, and M. Sintubin, Calcite textures: Example from nappes with strain path partitioning, *J. Struct. Geol.*, *13*, 369–384, 1991.

Simpson, C., Deformation of granitic rocks across the brittle-ductile transition, *J. Struct. Geol.*, *7*, 503–511, 1985.

Suppe, J., *Principals of Structural Geology.* 537 pp., Prentice Hall, Old Tappan, N. J., 1985.

Tobisch, O. T., J. B. Saleeby, P. R. Renne, B. McNulty, and T. Weixing, Variations in deformation fields during development of a large-volume magmatic arc, central Sierra Nevada, California, *Geol. Soc. Am. Bull.*, *107*, 148–166, 1995.

Wandres, A. M., S. D. Weaver, D. Shelley, and J. D. Bradshaw, Change from calc-alkaline to adakitic magmatism recorded in the Early Cretaceous Darran Complex, Fiordland, New Zealand, *N. Z. J. Geol. Geophys.*, *41*, 1–14, 1998.

Whitney, D. L., R. B. Miller, and S. R. Paterson, *P-T-t* constraints on mechanisms of vertical tectonic motion in a contractional orogen, *J. Metamorph. Geol.*, *17*, 75–90, 1999.

Williams, J. G., and C. T. Harper, Age and status of the Mackay Intrusives in the Eglinton-Upper Hollyford area, *N. Z. J. Geol. Geophys.*, *21*, 733–742, 1978.

Wood, B. L., Metamorphosed ultramafites and associated formations near Milford Sound, New Zealand, *N. Z. J. Geol. Geophys.*, *15*, 88–127, 1972.

G. L. Clarke and N. R. Daczko, School of Geosciences, University of Sydney, Building F05, NSW 2006, Australia. (geoffc@mail.usyd.edu.au; ndaczko@mail.usyd.edu.au)

K. A. Klepeis, Department of Geology, University of Vermont, Burlington, VT 05405-0122, USA. (kklepeis@zoo.uvm.edu)